ASPECTS OF MECHANICAL BEHAVIOR OF ROCK UNDER STATIC AND CYCLIC LOADING

Six Month Technical Progress Report
August 1971

by

B. C. Haimson and R. W. Heins
Co-Principal Investigators

Contract No. H0210004 - ARPA

94

ASPECTS OF MECHANICAL BEHAVIOR OF ROCK UNDER STATIC AND CYCLIC LOADING

SIX MONTH TECHNICAL PROGRESS REPORT
August, 1971

by

B. C. Haimson and R. W. Heins
Co-Principal Investigators

Department of Metallurgical & Mineral Engineering
and the
Engineering Experiment Station
College of Engineering
The University of Wisconsin
Madison, Wisconsin 53706

ARPA Order No. 1579, Amendment 2
Program Code No. 1F10
Contract No. H0210004
Contract Period: January 29, 1971 through January 28, 1972
Total Amount of Contract: $47,985
Sponsored by: ARPA

INTRODUCTION

This report describes our technical accomplishments during the first six months of the present contract. The report is in two parts. In Part A the results of a one-dimensional progression failure modeling of rock static behavior are described. In Part B our experimental findings in the mechanical behavior of rock under compressive cyclic fatigue are detailed. Part B is to be presented at the 13th Symposium on Rock Mechanics, Urbana, Illinois, September 1, 1971.

Work is now underway in rock tensile cyclic fatigue. A method has been found to test this fatigue behavior and preliminary results suggest that the concept of a fatigue limit for rock in tension is viable. A full account of our progress in this aspect of the program will be part of our next technical report.

PART A

A ONE-DIMENSIONAL PROGRESSIVE FAILURE MODEL OF ROCK

Robert G. Lundquist
Robert W. Heins

August, 1971

Department of Metallurgical & Mineral Engineering
The University of Wisconsin
Madison, Wisconsin 53706

TABLE OF CONTENTS

A ONE-DIMENSIONAL PROGRESSIVE FAILURE MODEL OF ROCK

Robert G. Lundquist
Robert W. Heins

ABSTRACT

It is well known that the strength and deformation properties of rock are highly variable. It has also been observed that rock does not fail in a weakest link manner but progressively, maintaining considerable load-bearing capacity beyond its peak load. It is hypothesized that the variability of properties and progressive failure behavior are direct consequences of the statistical inhomogeneity of the material. A one-dimensional model is used to demonstrate that progressive failure can indeed result from inhomogeneity of the material and to show what the effects of varying statistical distributions of properties might be on the gross deformation and failure of rock.

"You see, of course, if you're not a dunce,
How it went to pieces all at once, --
All at once, and nothing first, --
Just as bubbles do when they burst. "

The Deacon's Masterpiece
Oliver Wendell Holmes

CHAPTER I
INTRODUCTION

Problem Statement

In the interpretation of laboratory tests and in the design of structures in rock, we often assume that, like the Deacon's "wonderful one-hoss shay, " rock fails "all at once, and nothing first. " It is easily demonstrated that rock does not fail in this way under most practical loading conditions, and it is the purpose of this study to show the consequences of this misleading assumption and to present a simple model for rock failure which allows the interpretation of rock strength tests and the design of rock structures to be put on a more rational basis.

There are several implications in the idea of failing "all at once and nothing first" which we must examine. The first and most obvious is that once the strength of the material is exceeded by the stress, it is no longer capable of sustaining load. An abundance of recent evidence has shown, however, that in compressive and mixed stress fields, and in perhaps every loading except uniaxial tension, most rock can sustain considerable fractions of its peak load after this load has been exceeded. This is the concept of the "complete stress-strain curve, " perhaps more precisely called the "complete load-displacement curve" since only mean stress and strain can be determined after failure. It is this behavior which led Jaeger and Cook (1) to define the brittle state of a material as that condition in which "its ability to resist load decreases with increasing deformation. "

A second implication, which will be seen to be intimately connected with the first, is the idea of the "weakest link." By analogy to the ancient adage that a chain is no stronger than its weakest link, it is assumed that if failure ensues from exceeding the strength of any part of a rock structure, the entire structure will fail. Failure must here be defined as the loss of the entire load resisting ability of the structure. To see that this is untrue, we can examine some physical observations which have accompanied the production of complete stress-strain curves for rock in compression. Wawersik (2) found that visible cracks developed in a marble in uniaxial compression at about 90% of the ultimate load. At a displacement about 20% greater than the peak of the curve, the marble was capable of resisting about half of its peak load. Although many large cracks appeared, a major portion of the specimen was intact when it was unloaded from this point and removed from the machine. Some rocks, Wawersik's type II rocks, e. g., are indeed incapable of sustaining load beyond their peak. These rocks have a numerically positive "post-failure" slope so that self-sustaining failure can develop from only the elastic energy stored in the specimen and without additional energy from the machine. To test such rocks, it is necessary to remove energy from the rock in a controlled way after the peak is passed. In this limited case, rock fails in a weakest link way; however, it appears that the behavior is very dependent on loading conditions (3), and except as a nice explanation for rock bursts, it may not be applicable to rock structures at all. It cannot be generalized, then, that rock is a weakest link material in uniaxial compression. It should be obvious that in confined compression, rock sustains more load at greater displacement after the peak and is even less a weakest link material.

What about tension? Hudson, Brown and Rummel (4) have shown that discs and rings loaded in diametral compression (both considered to be indirect tensile tests) also produce a load-displacement curve in which

load is sustained at displacements beyond the peak. Again, visible cracks appeared while the specimen remained essentially intact. Again, one rock was found (Solenhofen Limestone) for which a complete curve could not be produced, but a weakest link model was not generally applicable.

Direct tension remains something of a mystery. Hughes and Chapman (5) showed a stable, bell-shaped curve for concrete, but to date, although there has been at least one serious attempt (6), no one has succeeded in publishing a similar result for rock. On the other hand, Brown and Singh (7) have shown that considerable acoustic energy is released at loads considerably below ultimate. Wawersik (2) found loosening of and fracture along grain boundaries well below the ultimate load and concluded that "Rock failure in tension can be a progressive process and does not necessarily occur suddenly. "

Even if we were to concede that indirect tension of a weakest link model is applicable, Hudson (8) has pointed out that direct tensile testing may not be applicable to the design of structures since in practice gradients will always be present.

The problem then, simply stated, is to make a quantitative model for rock which will allow progressive failure and residual strength to be interpreted in laboratory tests and then utilized in structural design.

> --"Fur, " said the Deacon, "t's might plain
> Thut the weakes' places mus' stan' the strain;
> 'N' the way t' fix it, uz I maintain, Is only jest
> T' make that place uz strong uz the rest. "
>
> The Deacon's Masterpiece
> Oliver Wendell Holmes

Inhomogeneity of Rock

The reason that the wonderful one-hoss shay went to pieces "all at once and nothing first, " Holmes tells us, was because of the deacon's rather exacting construction standards. He recognized the weakest link

concept and eliminated the problem by making each piece "uz strong uz the rest." One of the most obvious things about rock is that each piece is not "uz strong uz the rest." This is inhomogeneity.

The solution of most rock mechanics problems begins with a set of simplifying assumptions which are nearly universally acknowledged to be invalid. These assumptions usually include, but are not necessarily limited to elasticity (linear, small displacement elasticity up to failure), isotropy (two constant elasticity), time independence, and homogeneity.

As mathematical tools have become more generally available, these restrictive assumptions have been relaxed and we see today a hugh volume of literature treating rock as viscoelastic (especially valid for salt and potash), perfectly plastic or work hardening plastic (a good model for high confining pressure conditions as in deep sediments), transversely isotropic (useful for layered rocks), etc., etc. Inhomogeneity, however, has been largely ignored due to its severe insusceptibility to rigorous mathematical attack.

Since the term inhomogeneity seems to mean different things to different people, let us clarify what will be meant within the context of this study. By homogeneous, we mean that every point in a material, or at least in a particular specimen of that material, has the same properties as every other point. We must restrict the term "point" to the continuum mechanics sense and ignore the atomistic structure of the material. This condition of sameness of properties can be violated in several ways.

The most obvious kind of inhomogeneity is found when the specimen or region of consideration consists of two or more subregions with distinct properties. The example that comes most quickly to mind is a sandstone layer overlying a coal seam. A problem in this situation is deterministic in the same sense that any homogeneous rock mechanics problem is deterministic; the boundary conditions and material properties are or can be as well defined as in the homogeneous case. We will call this multiproperty, multiregion inhomogeneity <u>deterministic inhomogeneity</u>.

The second way in which the homogeneous sameness of properties condition can be violated occurs in a rock type (often thought of as a particular material) such as a conglomerate or large-grained granite, which is made up of two or more mineral constituents. The most obvious feature of such a rock, even to a layman, is its inhomogeneity. Unless we are forced by a particular test, such as an indentation test, to sample a very small volume of the rock, its inhomogeneity is usually shrugged off by calling it macroscopically homogeneous and assigning single values to its elastic and strength properties. For many purposes this is adequate; we will examine some of the consequences later. We will call this kind of inhomogeneity compositional inhomogeneity.

A more subtle violation of the sameness condition takes place in rocks composed of a single mineral, such as sandstone or rock salt. Here, properties vary from point to point, in spite of mineralogical sameness, because of the granular nature of the rock. Each grain is different. Each has its own unique orientation, which may or may not have a preferred direction. Each may contain flaws, such as cleavage or fracture, or impurities in varying amounts. Of equal importance is the difference in properties between the mineral grains and their boundaries. In our first course in geology, we are taught to differentiate between quartzite and sandstone on the basis of differing relative strengths of grain and grain boundary. How then can we consider these rocks homogeneous? Good engineering results to many problems can be had, however, by taking average or gross properties as before. This kind of inhomogeneity we label granular inhomogeneity.

There is, of course, no real separation between compositional and granular inhomogeneity, with most rocks possessing some degree of both. The important point is that this inhomogeneity is not deterministic. In a given problem, the boundary conditions and material properties are not well defined. There exists in such problems a degree of randomness. We will call this kind of randomness statistical inhomogeneity. It is

with the consequences and modelling of statistical inhomogeneity that we will be concerned.

The discussion of compositional and granular inhomogeneity might seem to imply that statistical inhomogeneity exists only on the scale of the grain size. This is useful in studying laboratory tests but becomes incomprehensible at the field scale. At this scale, deterministic inhomogeneity might include well defined stratigraphy and such structural features as faults, dikes, etc., or a particularly well mapped joint set. On the other hand, a joint set in which direction, spacing, and extent are known only approximately, as is the usual case, is an example of statistical inhomogeneity. Even within a single bed or mass of rock, a region may contain more or fewer flaws, more or fewer inclusions, or have a different mineralogical makeup from another region of the same bed or mass. Such variations may have trends which can possibly be accounted for in the model, but this variation can, in general, be said to make rock statistically inhomogeneous at the field scale.

Variability of Rock Properties

Virtually all researchers in rock mechanics are sufficiently aware of the statistical nature of rock to avoid drawing conclusions from the results of a single test. It can be argued, however, that the mean of a "sufficient" number of tests can be assigned as a "physical property" of rock. Since a mass of rock can be thought of as made up of an infinite number of such samples, its mean properties should be reasonably close to the mean of the sample properties and thus such properties we used in the design of structures in the rock mass. Such a practice obviously requires the use of a sizeable "safety factor." The difficulties involved in the use of safety factors will receive extended consideration in the section on reliability.

Many physical properties, including elastic constants, unit weight, porosity, permeability, thermal properties, etc., etc., have importance

in rock mechanics problems; all can be said to vary to greater or lesser extent from point to point within a rock mass.

Hudson (8) speaks of tensile strength variation being of three types:

(a) Variation with different specimens. If the same test is performed on the same rock under the same conditions, different values of tensile strength result.

(b) Variation with different specimen volumes. If the same test is performed on the same rock with specimens of different volumes, the average value of the tensile strength changes with volume.

(c) Variation with different tests. The average tensile strength varies with the type of test used. For example, the modulus of rupture can be twice the straight pull tensile strength.

While Hudson is referring only to tensile strength tests, his categories of variation are equally applicable to other strength measures. Within-test variation is a fact of all strength testing. We can expect considerably different average values for shear strengths determined by single shear, double shear and torsion tests. Brown, Hudson, Hardy, and Fairhurst (3) have recently shown that between-test variations can be expected with differing compressive strength tests as well.

Let us return now to the problem of using mean values from property tests as design values for strength. Within-test variations create a poorly recognized, but very serious problem in using test values for design. Given a weakest link model for rock failure, one should clearly take the minimum of a series of test results rather than the mean as a design value. Even without accepting weakest link failure, it would seem prudent to design for the worst condition likely to occur. This raises the question of whether or not rock has a minimum strength (other than zero). Particularly in tension it would seem likely that if sufficient specimens were tested, one would fail without application of any load at all. This, in turn, opens the much larger question of the sampling process itself. In selecting blocks of rock from the mass, coring specimens, sawing and

grinding them, we reject at each stage those samples which contain flaws. The resulting specimens can hardly be considered representative of the rock mass. It is for the foregoing reasons that rock is often considered to have no tensile strength at all in design problems.

The problem of a large number of specimens giving a zero minimum tensile strength is, of course, directly related to the size effect. The existence of a strength-size effect has been widely debated, and recent evidence (9) seems to indicate that what appears to be a size effect is attributable instead to stress gradient effects or perhaps to differing available energy of the testing machine in relation to energy required for failure of a given volume. If a size effect does exist, it probably is a nonlinear decrease in strength with increasing specimen volume. If the decrease persists to large volumes, design values of strength for rock structures must be correspondingly reduced. To apply laboratory observed size effects to large rock structures requires extrapolation over several orders of magnitude, which is always a questionable procedure.

One alternative appears to be in-situ strength testing involving very large specimen volumes. Disproportionate expense and the practical difficulties of performing such tests have limited their use.

Another alternative, which the progressive failure model described herein is intended to explore, is to make structural design problems as deterministic as possible by geologic mapping and extensive laboratory scale testing and to use the results of the laboratory testing to estimate distributions for the statistical variations in the properties.

Between-test variations raise the question of what test to use to obtain physical properties. Particularly in tensile testing there is a continuing proliferation of new tests and little agreement even on how to perform a single kind of test. It would seem that less attention should be paid to the question of which test and how to run it and more to the question of why different tests given different results. As an example,

Hudson, Brown, and Rummel (7) have recently shown that the Brazil (diametral compression) test, one of the most commonly used indirect tests for tensile strength, is not a tensile test at all. With the load surfaces in direct contact with flat steel platens (as the test is usually performed), they found that failure always initiated in the compressive zone underneath the loads. Even with the load surfaces protected, they could not cause failure to initiate at the center.

It can be readily assumed, but perhaps never proved, that the three types of strength variation above are manifestations of strength inhomogeneity. It is much easier to demonstrate that variations in other properties are directly related to statistical inhomogeneity of the material. The specific gravity of a rock specimen, for example, is clearly equal to the weighted mean of the specific gravities of all of its subregions (if proper account is taken of pore space). Similarly, the overall stiffness (EA/L) of a uniformly stressed specimen can be found by a finite element representation with each element given an independent modulus corresponding to the region it represents.

Probabilistic Failure Theory

All of the above-mentioned types of strength variation can theoretically be accounted for by a model which predicts not a unique failure stress but a probability of failure at any stress level. The best known of these models is Weibull's statistical theory of material strength (10, 11). While Weibull's theory has been shown to be inadequate for rock, probably because it is a weakest link theory, it will be useful to examine it here. The presentation here is due to Hudson (8) but is available from many other sources.

In its simplest form, Weibull's model consists of V elements, each having a probability of failure Po at a given stress σ. The probability of element survival is 1-Po, and the probability of system survival is $(1-Po)^V$.

If Pv is the probability of system failure, then

$$1 - Pv = (1 - Po)^V$$

or

$$Pv = 1 - \exp [V \log (1 - Po)] .$$

Weibull defines the risk of failure R as $- V_{\log} (1-Po)$. Since log (1-Po) depends only on the stress σ, the risk of failure of a differential volume element dv can be written as:

$$dR = F(\sigma)\, dv .$$

If we take $R = \int_V f(\sigma)dv$, then the probability of the entire specimen failing is:

$$Pv = 1 - \exp[- \int_V f(\sigma)\, dv]. \qquad (1-1)$$

The problem here is clearly that of defining $f(\sigma)$ so that the correct cumulative distribution of strengths (Pv vs. failure load curves) will result for each test and specimen volume. The function $f(\sigma)$, if properly chosen, would then be a "true" material property.

While the theory itself is independent of the mechanism of failure, it might be thought of in terms of a volume element containing a flaw which is "critical" (in the Griffith sense) at the particular level of normal stress to which the volume element is exposed. There is no reason to suppose that the distribution of flaws (or elemental strengths) is well described by any commonly used probability distribution. Weibull assumed that $F(\sigma)$ was given by:

$$f(\sigma) = \left[\frac{\sigma - \sigma_u}{\sigma_o}\right]^m \qquad (1-2)$$

where σ_u represents a stress below which no element failure can occur and σ_o and m are material constants. He later described it as "A statistical distribution function of wide applicability," and indeed it is. This function has been used in such diverse fields as econometric modeling, and the reliability of electron tubes.

Substituting (2) into (1), we obtain

$$P_v = 1 - \exp\left[-\int_V \left[\frac{\sigma - \sigma_u}{\sigma_o}\right]^m dv\right]. \qquad (1\text{-}3)$$

This is the basic equation of Weibull's theory. If the three constants are truly material constants, and can be found for a given material, Eq.1-3 can be integrated to provide a distribution of failure strengths (in terms of failure probability at a given stress) for any test or any specimen volume. The process can be quite involved since it requires knowing and integrating the stress distribution over the entire specimen volume. Nonetheless, it has been integrated for a number of tests. In his first paper, for example, Weibull presents the result that the modulus of rupture (3-point bending strength) is $(2m + 2)^{1/m}$ times the direct pull tensile strength. For $m = 3$, this factor is 2.0, and for $m = \infty$, the factor is 1.0 (the strengths are the same).

Since its publication in 1939, Weibull's theory has been widely discussed and the probability distribution widely employed. It has, however, been subjected to remarkably few experimental analyses. In many cases, experimental "verification" has consisted simply of finding a set of parameters, σ_o, σ_u, and m, to fit a given set of data. The existence of each parameter, of course, can neither prove nor disprove the theory.

It would be surprising, in fact, if a set of data derived from any statistical process could not be fit by a 3-parameter model. The usefulness of the distribution to describe the fiber strength of Indian cotton, statures for adult males born in the British Isles, and the breadth of beans of Phaseolus Vulguris, lies in its ability to "simulate" a wide range of more conventional distributions such as exponential, normal, and log-normal, as well as less common shapes.

Where the theory has been tested, particularly in rock, the results were poor. Hudson (8) found that the theory would not predict either the

effect of changing dimensions or the between test variations in 3 and 4 point bending sufficiently well.

There are two entirely independent reasons why Weibull's theory might not work. The first lies in the theory used in deriving equation 1-1. Only if failure initiation in any volume element tends to cataclysmic structural failure with no increase in stress can equation 1-1 be considered valid. We have previously seen that rock is not a weakest link material under common loading situations. Equation 1-1 cannot, then, be properly applied to rocks.

The second reason for the failure of the theory is in the choice of F(x). The function is a material property for any weakest link material. There is no justification at all for selecting the Weibull function, and thus no reason to expect that the constants are material properties. The application of equation 1-3 to any material is simply a curve-fitting process, in the same sense as polynomial curve fitting to physical or other data. It may be convenient computationally but putting physical interpretation on the three Weibull's material constants is as risky as interpreting the coefficients of a curve fit polynomial.

Even if we reject Weibull's theory as inadequate, it points up at least one indispensable fact: in interpreting laboratory strength test and designing rock structures, we cannot use strength deterministically. We must instead look for and design to a <u>probability</u> of failure.

Reliability

Quite naturally, the vocabulary and much of the mathematics dealing with the probability of failure are found in the literature of reliability. Unfortunately, workers in reliability are usually concerned with the probability of element or system failure as a function of time, without regard to whether it is load or strength or both which change with time or are probabilistic functions of time. Two concepts from basic reliability theory are important here: chain reliability and redundancy.

Chain reliability is represented by a series circuit (Fig. 1-1) in which each element must remain unfailed for the system to be unfailed.

FIG. 1-1 Chain Reliability

If Px is the probability that element x is unfailed, then qx = 1 - Px is the probability that element x is failed. The reliability R of the system is

$$R = P_A P_B P_C P_D P_E$$

The probability of system failure Q = 1 - R is then:

$$Q = 1 - P_A P_B P_C P_D P_E$$

We previously encountered the same notion in the derivation of Weibull's theory where by taking the probability of failure ($P_o = 1 - P = q$) as the same for all elements, we found the probability of system failure $Q = 1 - (1 - P_o)^V$ for V series elements.

Redundancy is represented by a parallel circuit (Fig. 1-2) giving the opposite formulation. Here it is assumed that if any element is unfailed, the system is unfailed.

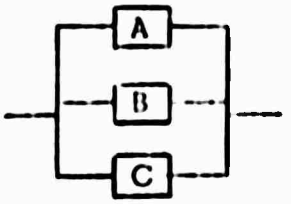

FIG. 1-2 Redundancy

Taking qx as the probability of element failure as before, we have

$$Q = q_A q_B q_C$$

and

$$R = 1 - Q = 1 - q_A q_B q_C$$

The resulting Weibull type model for the redundant material would have:

$$P_v = (P_o)^v = \exp [v \log (P_o)].$$

Given again that $P_o = qx$ is a function of the stress, we could write

$$P_v = \exp [\int_v f'(\ ) \, dv]. \qquad (I-4)$$

We would again be faced with the problem of finding $f'(\ )$ for the material in question.

Notice that equation I-4 describes a material which loses no strength with element failure while the Weibull weakest link material lost all of its strength with element failure. The redundant material is clearly a poorer model for rock than the weakest link material; the truth is somewhere in between.

Another approach to probability of failure, which we shall find extremely useful, is that taken by Kececioglu and Cormier (12). They determine the probability of failure of a structural component by assuming that it is equal to the probability that a statistically distributed stress exceeds a statistically distributed strength. They enumerate a large number of factors which cause both stress and strength to be probabilistic rather than fixed quantities. They recommend finding a failure governing stress for the component and modifying the nominal stress at the probable failure point by various factors using Monte Carlo for all variables concerned to produce an empirical frequency distribution for stress. Similarly, an empirical distribution could be constructed for strength by starting with the nominal (handbook) strength of the material. They say little about finding the distributions of the individual variables making up the stress and strength distributions but indicate that the strength distribution can be found by testing a number of actual components under the actual environmental conditions of their use. This would leave only the load

distribution and certain environmental factors in the stress distribution.

Kececioglu and Cormier show how to compute reliability R or the probability of component failure Q (= 1 - R) from the distributions of strength (S) and stress (s). If f(S) and g(s) are probability density functions as shown in Fig. I-3, then the probability that stress is in the interval ds about S_1 is area A_1.

$$P(s_1 - \frac{ds}{2} \leq s \leq s_1 + \frac{ds}{2}) = g(s_1)\, ds = A_1$$

The probability that S > s is the shaded area under the strength density curve A_2.

$$P(S > s_1) = \int_{s_1}^{\infty} f(S)\, dS = A_2$$

The probability of no failure, i. e., the reliability, at s_1 is the product of these two probabilities.

$$dR = g(s_1)\, ds \times \int_{s_1}^{\infty} f(S)\, dS$$

Reliability of the component is the probability of the strength exceeding the stress over the entire range of applied stresses:

$$R = \int dR = \int_{-\infty}^{\infty} g(s) \left[\int_{s}^{\infty} f(S)\, dS \right] ds \qquad \text{(I-5)}$$

An alternative formulation can be found from the probability that stress is less than strength:

$$R = \int_{-\infty}^{\infty} f(S) \left[\int_{-\infty}^{s} g(s)\, ds \right] dS \qquad \text{(I-6)}$$

By using the properties of density functions:

$$\int_{-\infty}^{\infty} f(S)\, dS = 1$$

and

$$\int_{-\infty}^{\infty} g(s)\, ds = 1$$

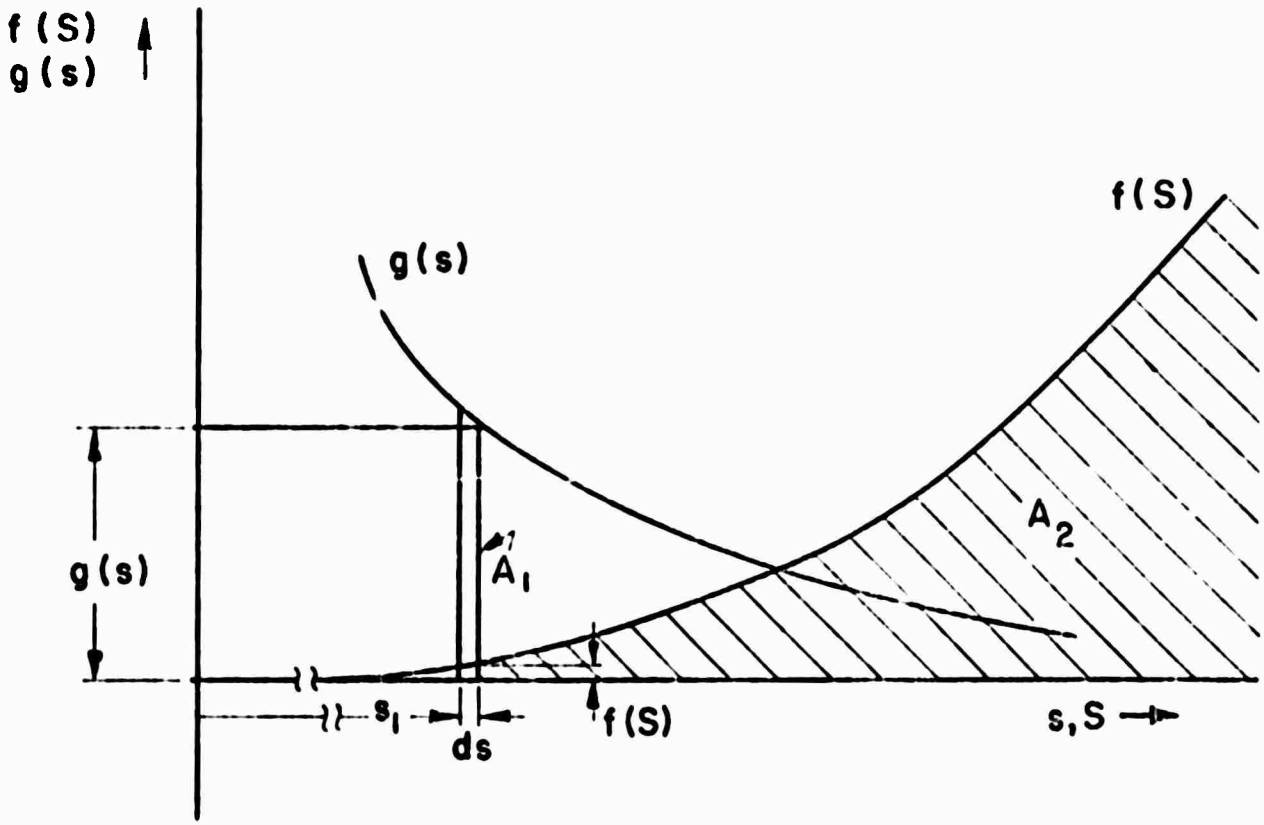

FIG.- I - 3 GENERAL STRESS & STRENGTH DISTRIBUTIONS

it can presumably be shown that I-5 and I-6 are equal.

Equations I-5 and I-6 can be readily solved numerically. Exact solutions for common probability functions are obviously much more difficult. By using an alternate approach, Kececioglu and Cormier give the exact solution for the case where both stress and strength are normally distributed.

The density functions for the normal distributions are:

$$g(s) \quad \frac{1}{\sigma_s \sqrt{2\pi}} \exp\left[-\frac{1}{2}\left(\frac{s-\bar{s}}{\sigma_s}\right)^2\right]$$

and

$$f(S) \quad \frac{1}{\sigma_S \sqrt{2\pi}} \exp\left[-\frac{1}{2}\left(\frac{S-\bar{S}}{\sigma_S}\right)^2\right]$$

where $\bar{S}$ and $\bar{s}$ are the means and σ and σ_S are the standard deviations.

Reliability is the probability that strength exceeds stress or that $S - s > 0$. Taking $S - s = \zeta$, reliability is the probability that $\zeta > 0$. The distribution of ζ, called the difference distribution, is also normal and is thus:

$$h(\zeta) \quad \frac{1}{\sigma_\zeta \sqrt{2\pi}} \exp\left[-\frac{1}{2}\left(\frac{\zeta-\bar{\zeta}}{\sigma_\zeta}\right)^2\right] \tag{I-7}$$

where $$\bar{\zeta} = \bar{S} - \bar{s}$$

and $$\sigma_\zeta = \sigma_S^2 + \sigma_s^2$$

Reliability R is given by the positive density of ζ. Thus:

$$R = P(\zeta > 0) = \int_0^\infty h(\zeta)\, d\zeta \tag{I-8}$$

The probability of failure Q (1 - R) is given by:

$$Q = P(\zeta < 0) = \int_{-\infty}^0 h(\zeta)\, d\zeta \tag{I-9}$$

This is the shaded area in Figure I-4. The solution to equation I-8 or I-9 can be found from tables for the standard normal distribution by first making the transformations of mean and standard deviation indicated by equation I-7.

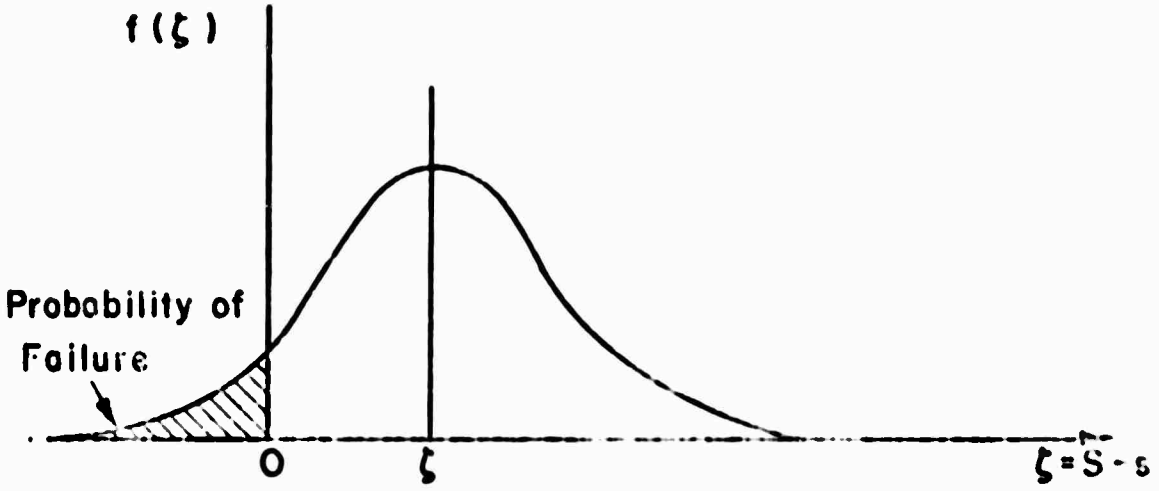

FIG.1-4 DIFFERENCE DISTRIBUTION

The problem of approximating stress and strength by normal distributions remains. Without presenting the justification in detail, Kececioglu and Cormier suggest that normal distributions can be approximated from pessimistic, most likely, and optimistic estimates of strength or stress. If we take a, b, and c as the three estimates then:

$$s = \frac{a + 4b + c}{6}$$

$$\sigma_s = \frac{c - a}{6} \qquad (I\text{-}10)$$

are considered good approximations. They are based on the optimistic and pessimistic estimates being three standard deviations above and below the mean, respectively. The weights might need to be different but the concept is highly applicable to structural design in rock and is, as we shall see, very much preferable to the use of safety factors.

The safety factor is defined as the ratio of strength to stress. By taking the ratio of the mean values of the distributed stress and strength as a safety factor, Kececioglu and Cormier point out some fallacies in the use of safety factors for design.

Designers generally believe that a safety factor above some preconceived value (for example, four to eight for rock in tension) will result in no component failure. On the contrary, with these or even higher safety factors, there exists some finite probability of failure which might vary from acceptably low to intolerably high. Similarly, it is commonly believed that a safety factor of one will result in certain failure. In fact, if stress and strength distributions are normal (or any symmetric distribution), a safety factor of one gives a probability of failure of 0.5 regardless of the standard deviations involved. Even a safety factor less than one does not result in certainty of failure.

Kececioglu and Cormier point out two ways in which failure probabilities might vary with a constant safety factor.

1. The mean of the stress and strength distribution can be changed in the same proportion with fixed standard deviations. If both are increased, the probability of failure decreases and vice versa.

2. The standard deviations can be altered while keeping the means fixed. In this case, an increase of one or both standard deviations increases the probability of failure.

They quote examples where with a constant safety factor of 2.5, the reliability of a component might range from .6628 up to $1-10^{-16}$.

Finally, it should be noted that Haugen (13) has written a book detailing ways for design of mechanical and electromechanical devices by this method.

CHAPTER II

A ONE-DIMENSIONAL MODEL

Hudson's Model

The chief criticism of the Weibull theory, insofar as its application to rock is concerned, is that it is a weakest link model. An attempt to formulate a Weibull-type treatment based on a redundant model gave an unacceptable result because it allowed for no deterioration with element failure, creating a sort of strongest link model.

A simple, mathematically elegant one-dimensional model which allows for structural deterioration with element failure has been constructed by Hudson (8). This model makes use of distributions of stress and strength in a manner strikingly similar to Kececioglu and Cormier's reliability computation. There is an important difference, however. Rather than being concerned with probability of failure of an entire component, Hudson's model looks at the probability of failure of an infinitesimal element, and deteriorates the structure in a systematic way as each element fails.

The model is most easily visualized as a large number of parallel elements, similar, as Hudson points out, to the springs in a mattress.

Hudson works entirely in terms of strain rather than stress, and further assumes that the assemblage is to be tested in a "stiff" (strain-controlled) machine.

As the assemblage is loaded, a mean strain (disturbance) is applied to the specimen. The strains on each element, however, are assumed to be distributed about this mean. Hudson, as did Kececioglu and Cormier, assumes a normal distribution for illustration; the model is not, however,

dependent on the choice of distribution. He assumes that each element is linearly elastic until its strain reaches a certain value, at which failure occurs and the element can no longer sustain load. As the specimen is loaded by the strain-controlled machine, the mean strain is presumed to increase monotonically, i.e., it is the independent variable and the total load or stress on the assemblage is the response.

Hudson unaccountably takes the variances of the two distributions as:

$$\sigma_d^2 = \bar{\epsilon}_d/x^2 \quad \text{and} \quad \sigma_s^2 = \bar{\epsilon}_s^2/l^2 \ .$$

The effect of this assumption is that as $\bar{\epsilon}_d$ is increased through the test, the variance of the ϵ_d distribution also increases. Note that ϵ_s remains constant so that the assumption that variance is a function of mean value has no effect. The quantity $\bar{\epsilon}_s^2/l^2$ is simply an arbitrary constant.

Hudson points out that x and l should be chosen so that $\bar{\epsilon}_d$ and $\bar{\epsilon}_s$ are always greater than three standard deviations away from zero. This will reduce the number of negative strains and strengths to about 0.13% of the total. Unbounded distributions have the slight disadvantage of always producing some negative values. Because standard deviation is the square root of the variance, the requirement is satisfied by x and l themselves exceeding three.

As $\bar{\epsilon}_d$ is increased, elements fail in succession; failure occurs in each element when $\epsilon_d > \epsilon_s$. At any value of $\bar{\epsilon}_d$, the probability of failure is given by the difference normal distribution as shown by Kececioglu and Cormier.

Hudson next makes the crucial assumption that the resistance of the overall assemblage is proportional to $1(\bar{\epsilon}_d)$, the "survival function" or proportion of elements unfailed at any $\bar{\epsilon}_d$. Thus:

$$\bar{\sigma}_r = C\, 1(\bar{\epsilon}_d)\, \bar{\epsilon}_d \qquad \text{(II-1)}$$

where $\bar{\sigma}_r$ = mean stress response

and C = a constant of proportionality.

As $\dot{\varepsilon}_d$ approaches zero, the survival fraction I approaches one, thus the constant C is the tangent modulus at zero load or Young's Modulus of the material. The quantity C I is the relation between stress and strain at any point and is therefore the secant modulus.

Resulting theoretical stress-strain curves for the assumption that k - 1 are shown in Figure II-1. In general shape, these curves bear a marked similarity to complete stress-strain curves for rock in compression. Note also that for k - 1 = ω, the "perfectly homogeneous" case, the stress drops instantaneously to zero and the model represents a weakest link material.

The behavior shown in Figure II-1 can best be described as "progressive failure" or, as Hudson puts it, "structural breakdown." Clearly, such a process represents an apt way to describe the way rock fails.

Development of a Numerical Model

In order to investigate some of the ramifications of Hudson's model, a discrete numerical model was constructed and programmed for the digital computer.

There are a finite number of elements N arranged in parallel as before. It is customary in rock mechanics work to use original specimen dimensions in computing stress and strain. The increase and later reduction of area in a compression specimen is ignored and strain is taken as "engineering" rather than "true" strain. The model can be simplified, therefore, without sacrificing generality, by working in terms of force and displacement rather than stress and strain.

Hudson assumes that the reduction in stiffness as each element fails is a constant. The total stiffness K of a collection of parallel elastic elements is the sum of element stiffnesses k_i, thus:

$$K = \sum_{i=1}^{N} k_i \qquad NK \ .$$

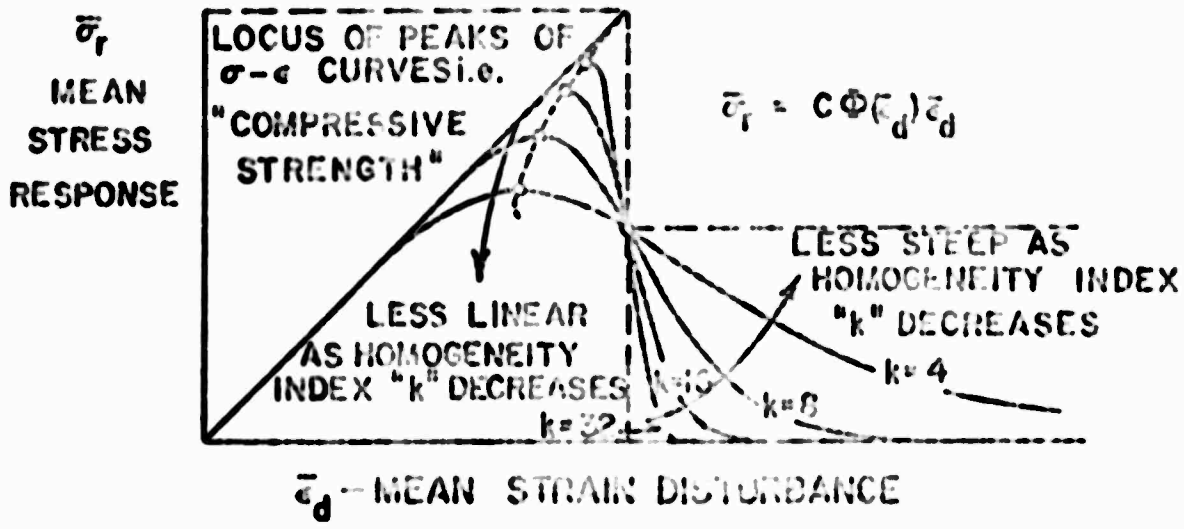

FIGURE I-1 STRESS-STRAIN CURRES FOR HUDSON'S MODEL

The total force F on the assemblage is:

$$F = \sum_{i=1}^{N} f_i = \sum_{i=1}^{N} k_i \zeta_i = N \bar{\zeta}_i K \qquad \text{(II-2)}$$

where ζ_i = the distributed element displacement

and $\bar{\zeta}_i$ = the mean element displacement.

As the distribution of ζ_i is increased, propagating the disturbance into the assemblage, the individual ζ_i will begin to exceed the distributed strengths ε_i. We will assume that they lose their load bearing capacity as before and that we should deal only with the number of unfailed elements n where:

$$n = l\ N \qquad \text{(II-3)}$$

and l is the survival fraction.

Combining equations II-2 and II-3, we get:

$$F = n k \bar{\zeta}_i = l\ n k \bar{\zeta}_i = l\ K \bar{\zeta}_i \qquad \text{(II-4)}$$

which is Hudson's equation (II-1) in terms of force and displacement. Note that l is again a function of the difference distribution, this time of $(\bar{\zeta}_i - \bar{\varepsilon}_i)$. In equation II-4, K is the initial stiffness or tangent stiffness and l K is the secant stiffness.

Let us first ask what would happen if we were to distribute forces rather than displacements. The element displacements would still be distributed in the same way since $f_i = k \varepsilon_i$ and equation (II-4) would still ensue. The survival fraction would still be the result of the difference distribution and the form of the resulting stress-strain curves would be unaltered.

The result is rather surprising since the form of the complete stress-strain curve is rather different in a load-controlled (soft) machine. We see, however, that working in terms of force has not modeled soft loading at all since it is f_i that is increased monotonically and not F.

To make Γ the independent variable, we need a rule for distributing f_i among the surviving elements so that $\Gamma = \sum_{i=1}^{n} f_i$. With our previous assumption that all k_i were the same, the simplest rule is to make all $f_i = \frac{\Gamma}{n}$ and thus $\delta_i = \Delta$. This simply says that the progressive failure of the material results entirely from inhomogeneous strength.

Two other ways are apparent. The first is to keep $k_i = k$ and to assume that differing f_i's result from a distribution of initial displacements. We must have $\bar{\delta}_o = 0$ so that $\Gamma = 0$ at $\Gamma = 0$. Then, $f_i = k(\delta_i + \delta_o)$. This could also be represented as an initial force distribution $f_i = k\delta_o$. The assumptions that $k_i = k$ and of initial forces or displacements are physically less appealing than the second possibility. Here we assume that the distribution of f_i results from a distributed k_i and that all $\delta_i = \Delta$.

The second approach was chosen for programming to test the effect of the distribution shape and size on the resulting stress-strain (actually force-displacement) curves. Hudson had compared the results of using both distributions normal and both uniform and found that the curves were almost indistinguishable. This was thought to be inconclusive, however, and the five bounded distributions discussed in Appendix A were programmed so that the stiffness and strength distributions could be selected with any shape, any mean, and any width or variance desired.

The model was first programmed with a force failure criterion and arranged so that for a given set of data, generated by Monte Carlo from the selected distributions, both force and displacement loading results were plotted. Since the compatibility equation says that all $\delta_i = \Delta$, the force f_i on an element is $f_i = k_i\delta_i = k_i\Delta$. Failure occurs when $f_i = s_i$, the strength of the element (now in force terms). The order of failure is thus determined by the ratio s_i/k, which is actually the failure value of Γ_i. We see that the supposed force failure criterion has become a displacement failure criterion due to the restrictions of the model. This approach was tried with interesting results, but it was discovered that the ratio of two random variates, even from the simple uniform distribution, has a complex

distribution which makes physical interpretation of the effects of distribution shape and size rather difficult. A second version of the program was written in which the displacement failure criterion was generated directly.

Let us now look at the workings of this program. The number of elements is read in along with the shape and variance of the distributions. Subroutines are called which generate a stiffness and a strength value (now in displacement units) for each element. The elements are then sorted and renumbered in order of increasing failure displacement and the total stiffness of the assemblage is computed. In displacement loading, the total force is calculated from the given displacement and the total stiffness; the stiffness of the failed element is subtracted to obtain the new total stiffness and the process is repeated. The arrays containing total force and corresponding displacements are saved and can be printed out or plotted or both.

Force loading requires only a slight modification of the displacement procedure. At each step, a check must be made to see if the failure of one element has redistributed forces in such a way as to cause failure of additional elements. With a force failure criterion this can be done by direct comparison of new element force to strength. It is much simpler (and more easily adapted to displacement failure), however, to check for a drop in total force at each step. If such a drop occurs in the displacement loading, it is ignored in force loading and the previous force substituted.

Since drops in force are always small and localized phenomena on the rising side of the force displacement curve, the two methods tend to give nearly identical plots up to the peak of the curve. After the peak is passed, the force loading curve merely displaces without limit at a constant force and is uninteresting. After some testing of these facts, the computing and plotting of the force loaded curve were discontinued. The final version of the one-dimensional program is presented in Appendix B.

We note that the plotted path does not agree in detail with either the force loading path or the displacement loading path. The drops in force in the displacement loading path become very small unless the drop in stiffness is a large proportion of the remaining total stiffness as is grossly exaggerated in these examples. Deviations of the plotted path from the displacement loading path are therefore negligible in large assemblages of elements. Up to the peak of the curve only rather general drops in force will cause large deviations of the force loading path from the plot. Except where such a general drop might occur, it can be claimed that the plotted output fairly represents either force or displacement loading up to the peak of the curve.

The model, as developed above, can theoretically represent any rock loading situation in which stress gradients can be assumed negligible. This essentially precludes modeling all but uniaxial tension and compression tests.

To reduce the number of independent variables in the model and facilitate comparison between tests, a hypothetical rock was selected for modeling in a uniaxial compression test. The specimen is a cylinder with a diameter of 2 inches and a length of 4 inches. The rock has a modulus of 7.6×10^6 psi giving a stiffness $K = \frac{AE}{L}$ of 6×10^6 lbs. It has a yield point of 7600 psi or 24,000 lbs, and it has a strength of about 13,000 psi or 40,000 lbs.

Results

The one-dimensional model, as programmed in Appendix B, has a large number of independent variables. Clearly, a factorial design involving sufficient levels of all variables is out of the question; a systematic reduction was attempted instead.

The logical starting point is the number of elements N. It seems reasonable to assume that the effects of varying N will appear independently of the other variables in the model (i.e., the distributions). These effects

are of two distinct kinds. The least important, but probably most obvious in the figures which follow, is that the plotting of smaller numbers of points by a "connect the dots" rule will produce a jagged curve. More important is the statistical "law of large numbers" which says that if a "sufficient" number of samples is taken, the sample distribution is arbitrarily close to the theoretical distribution. This means that as N approaches infinity, the curve produced by the model becomes determinate. The number of elements should be selected large enough to make the force displacement curve smooth and reproducible.

This requirement must be balanced against the increased cost, in terms of computing time, of increasing N. Figures II-2 through II-6 show the results of varying N (N = 10, 100, 500, 1000) with both distributions uniform. The curves for N = 500 and N = 1000 are smooth and nearly indistinguishable, while the curves for N = 10 and N = 100 are rough and not reproducible. It was concluded that 500 elements were sufficient, and this number was used in most of the later trials.

Originally, testing was done with A_s, the lower bound of the strength distribution, fixed at .004 inch. This was to simulate a rock with a yield point of 24,000 lbs. or about 7,600 psi. The model is elastic until the first element fails which will occur at the displacement where the least strength is exceeded. The stiffness returns to zero when the last element fails, thus B_s represents a "maximum" displacement. The result of changing the variance of the strength distribution is shown in Figure II-7. Here the stiffness distribution was held constant while the variance of the strength distribution ranged from zero to 5.6×10^{-5}. Both distributions were uniform for this test. With bounded distributions the role of the strength variance, or specifically the upper and lower bounds of the strength distribution, is to fix the yield point and the maximum displacement at which the specimen can bear load. If A_s and B_s are coincident (variance = 0), the yield, peak and maximum displacement occur at the same displacement and weakest link failure occurs.

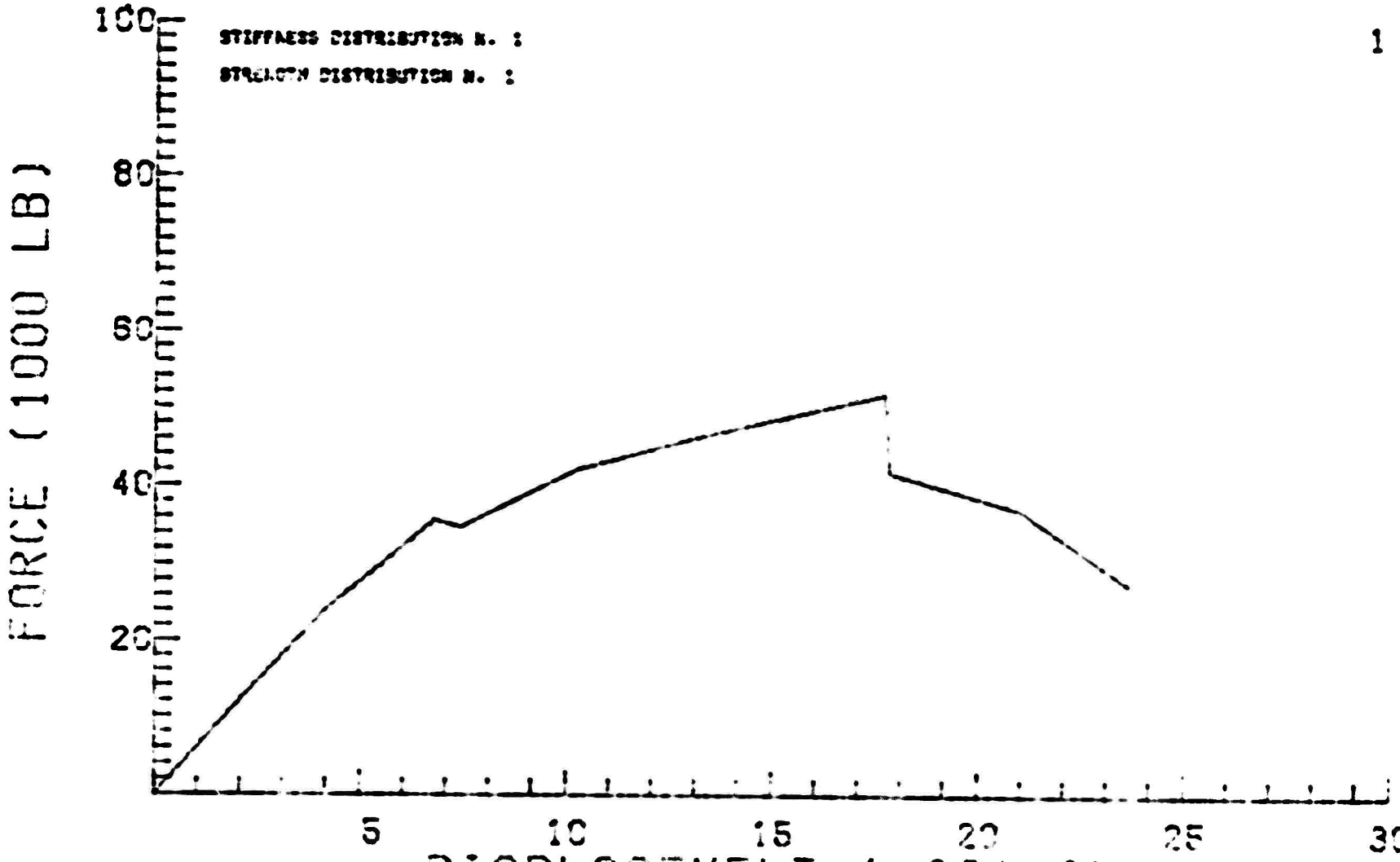

FIGURE II-2 Effect of N
N = 0

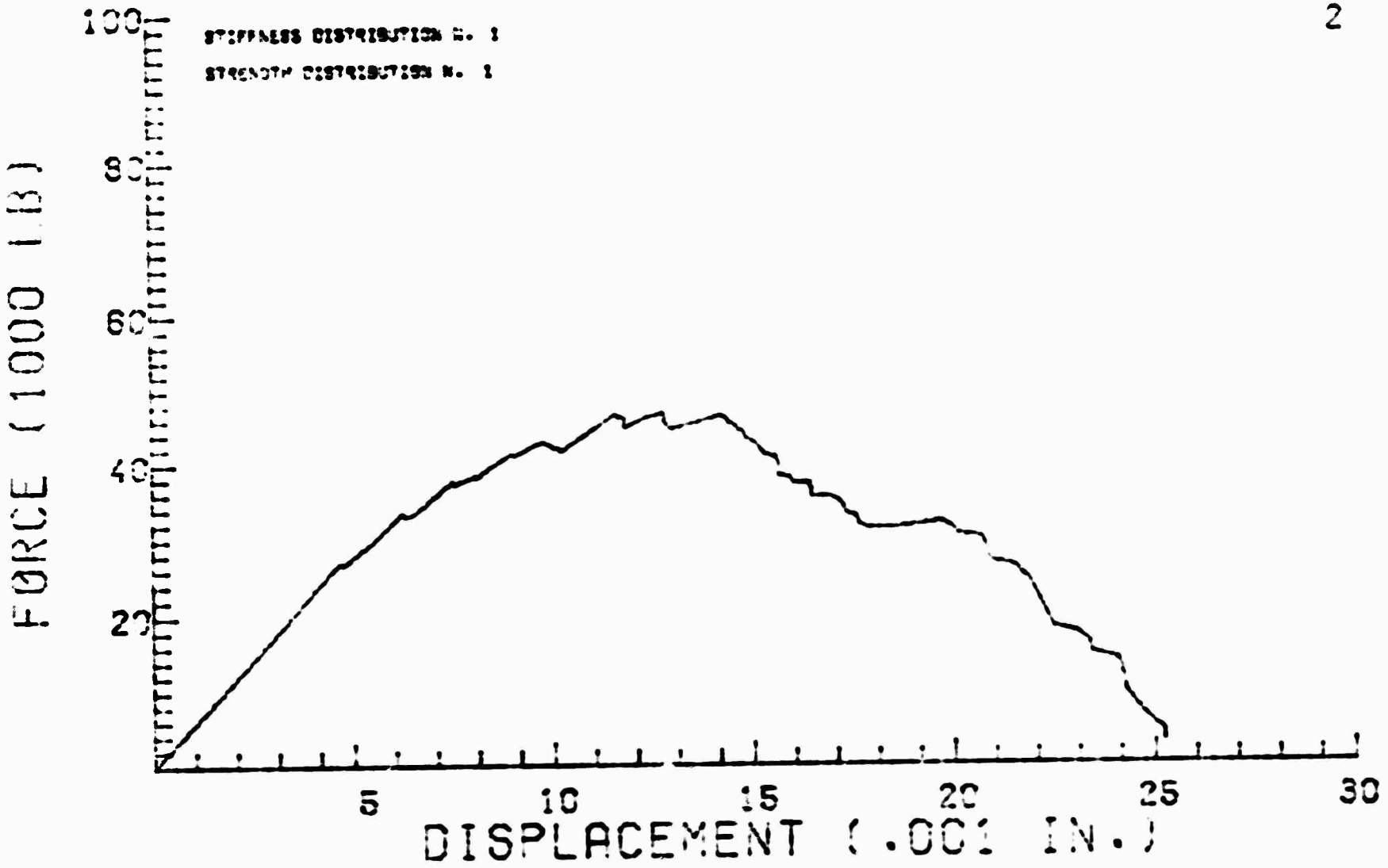

FIGURE II-3 Effect of N
N = 100

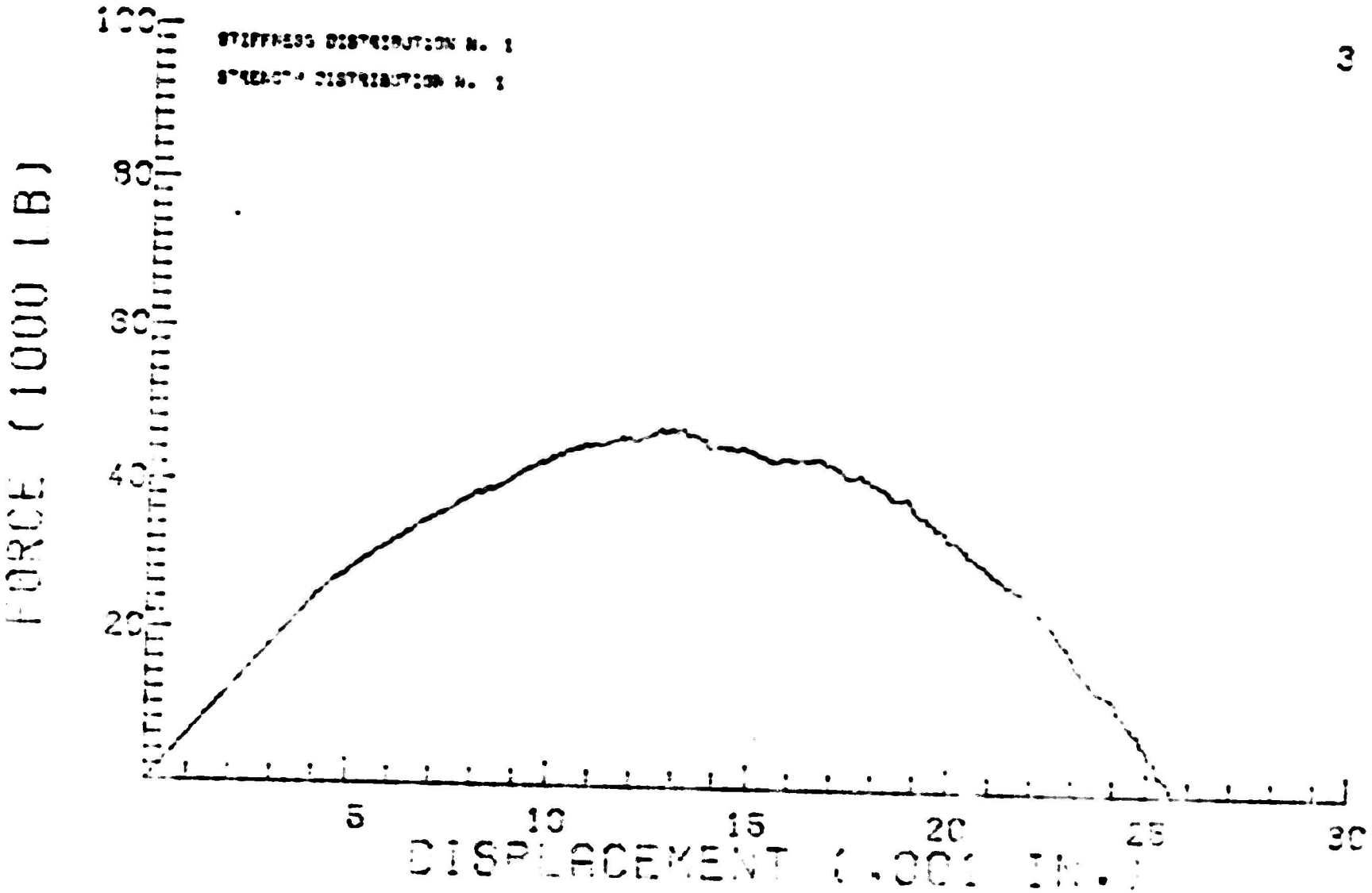

FIGURE II-4 Effect of N
N = 500

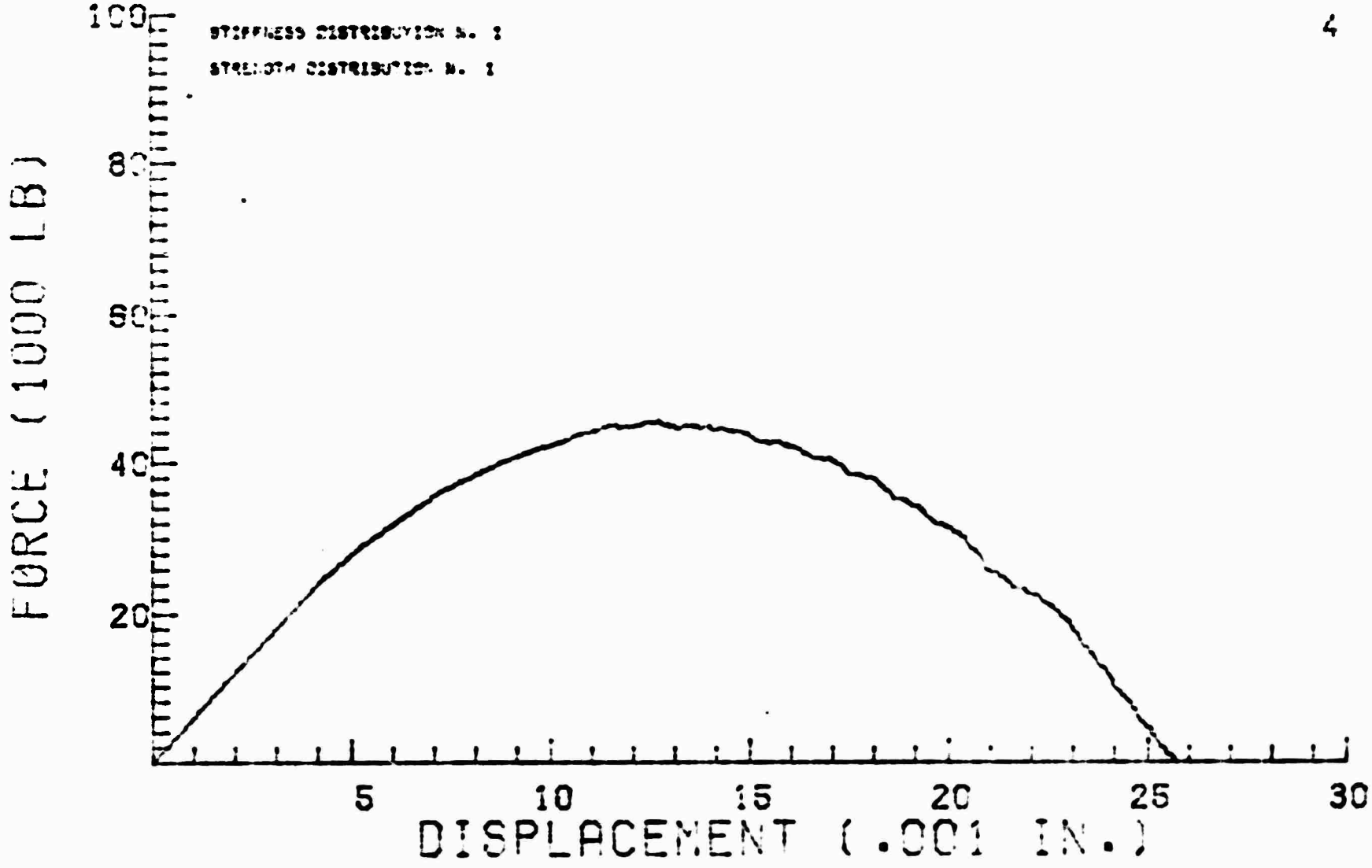

FIGURE II-5 Effect of N
N = 1000

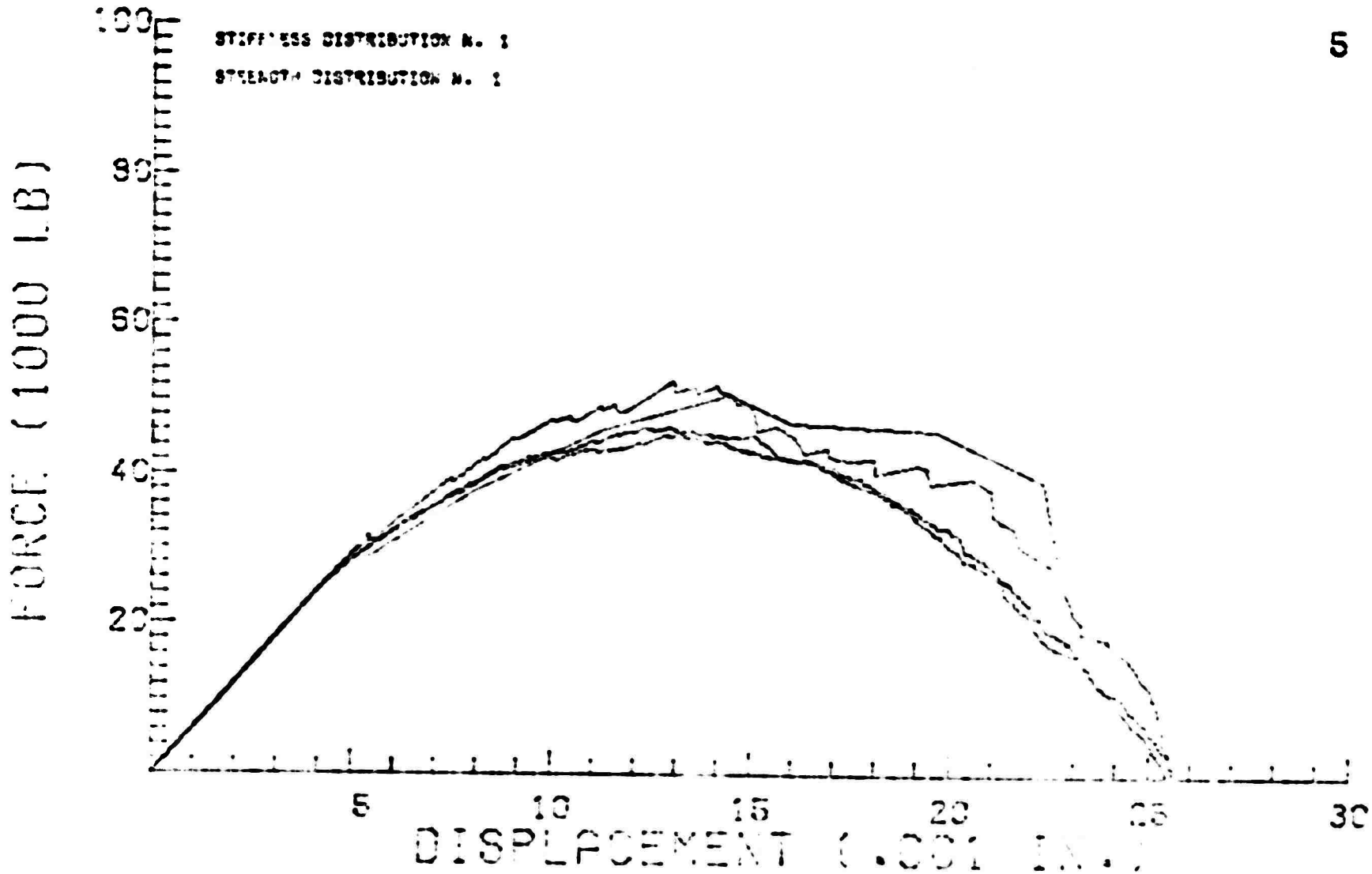

FIGURE II-6 Effect of N Compared
N = 10, 100, 500, 1000

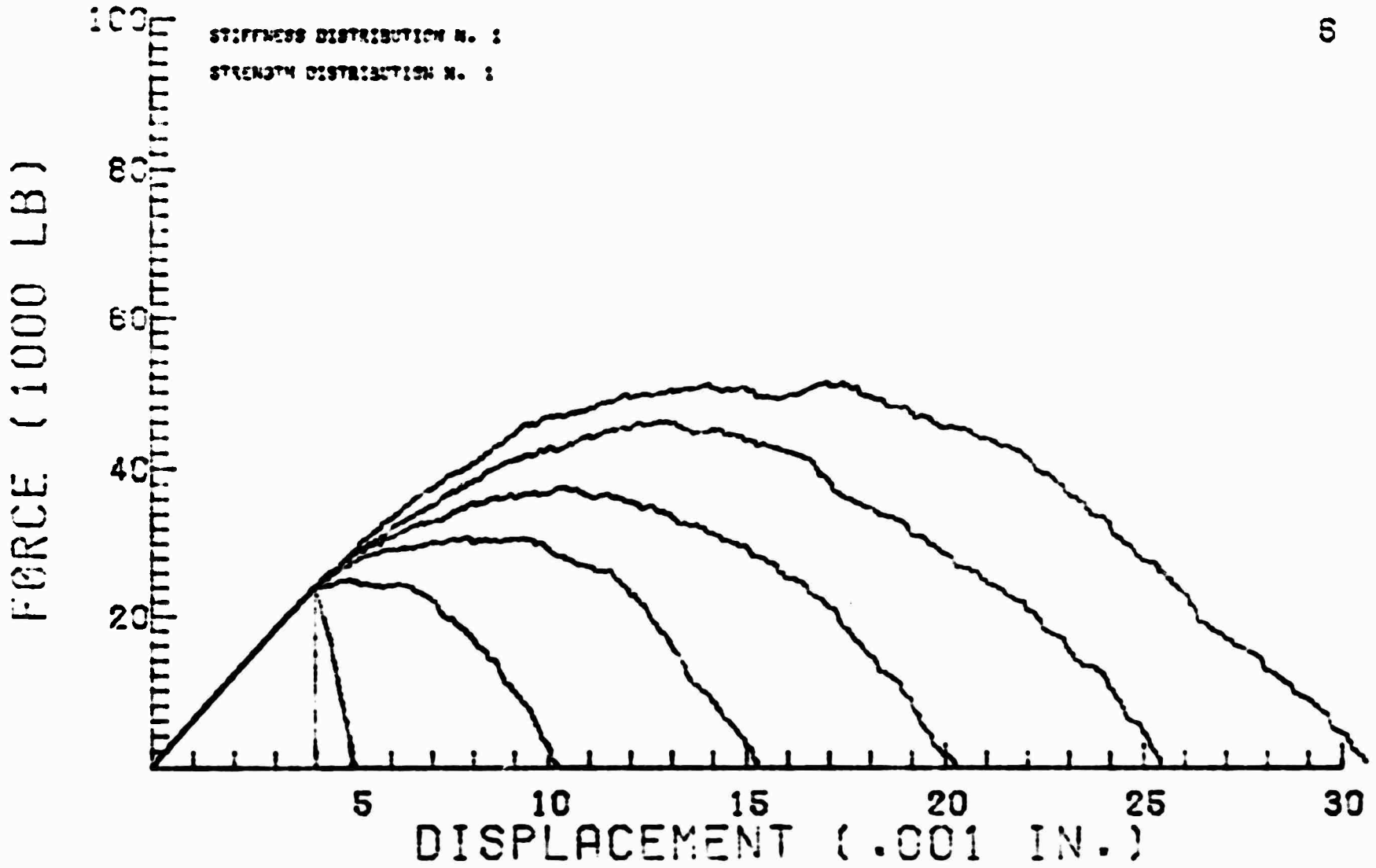

FIGURE II-7 Effect of B_s
B_s = .004, .005, .010,
.015, .020, .025, .030

The effect of V_K is shown similarly in Fig. II-8. Here V_K ranges from zero to 10 with both distributions again uniform. The curves are quite interchangeable. This unexpected result is due to the independence of the stiffness and strength distributions. In the program the strengths are sorted in order, but because it is independent the stiffness is still quite random. Over a large number of small displacement steps, therefore, the drop in stiffness at each step will tend to the mean of the distribution which is determined beforehand by selecting K. For a total stiffness of 6×10^6 lbs, each element has a mean stiffness of $6 \times 10^6/K$ lbs. The fact that the force displacement curve is independent of the stiffness distribution is again illustrated in Fig. II-9 where the strength distribution is again uniform and fixed and the stiffness distribution shape itself is varied. Again the curves are interchangeable.

Figures II-10 through II-14 show the effect of the five possible shapes of the strength distribution on the force-displacement curve. Figure II-10 shows the smooth, rather symmetrical curve produced by the uniform distribution. Fig. II-11, with the strength unimodally distributed, is still smooth but has a peak about one-third higher than Fig. II-10. This is because fewer elements fail in the early stages of displacement and the specimen retains more stiffness at higher displacements. Fig. II-12 shows a still higher peak caused by even less element failure at small displacements with the left skewed distribution. Fig. II-13 shows the opposite effect of the right skewed distribution where elements fail most rapidly in early loading and slower near the end, thus flattening the falling side of the face displacement curve. Finally, Fig. II-14 shows the behavior when the distribution is bimodal, causing a plateau effect in the middle range where few elements are failing.

Up to this point, the minimum of the strength distribution Δ_s was fixed at 0.004 inch. In Fig. II-15, its effect is analyzed independently with the strength distribution uniform and the minimum strength Δ_s varying from 0 to 0.008 inch and the strength variance held constant.

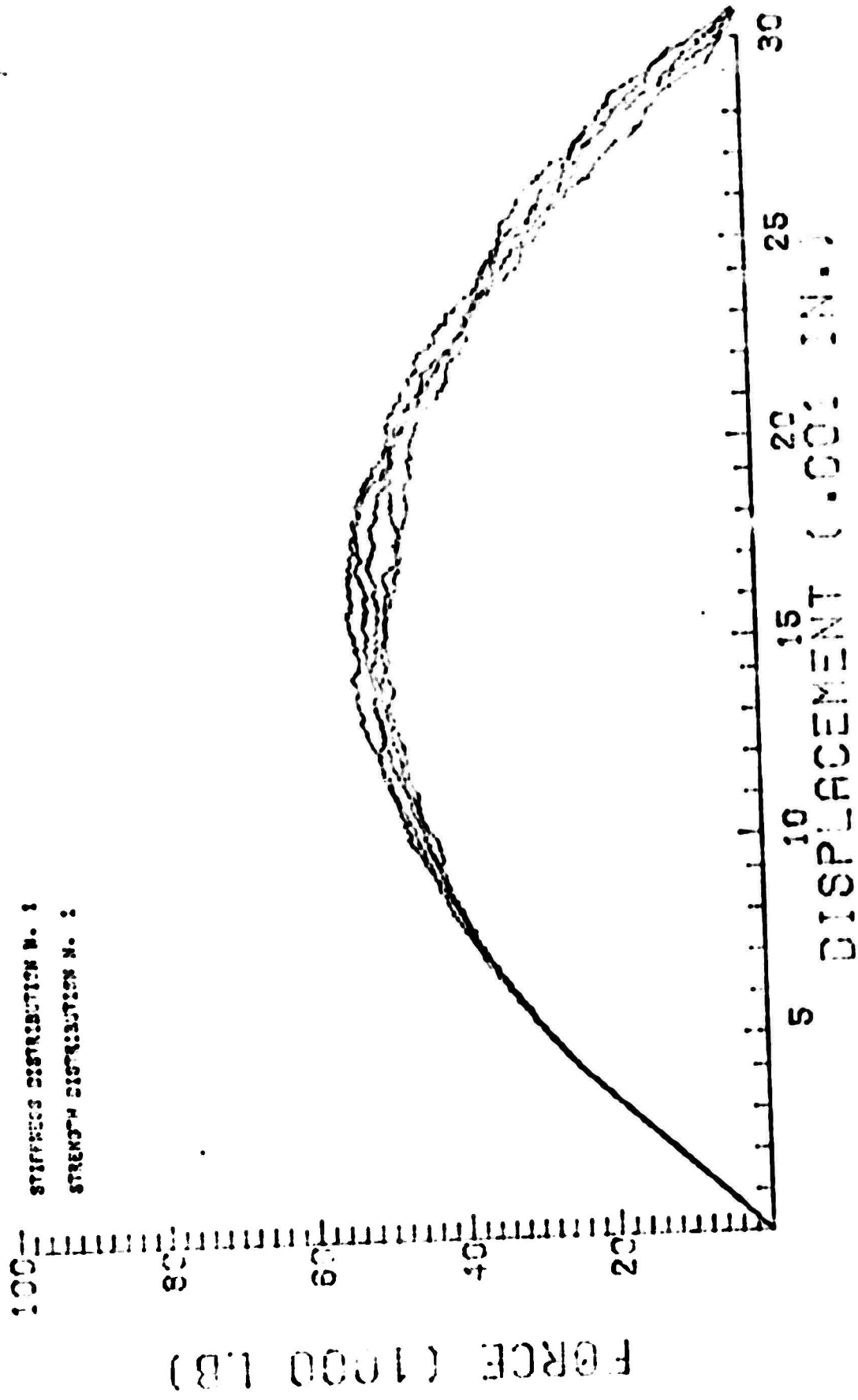

FIGURE I-8 Effect of V_K

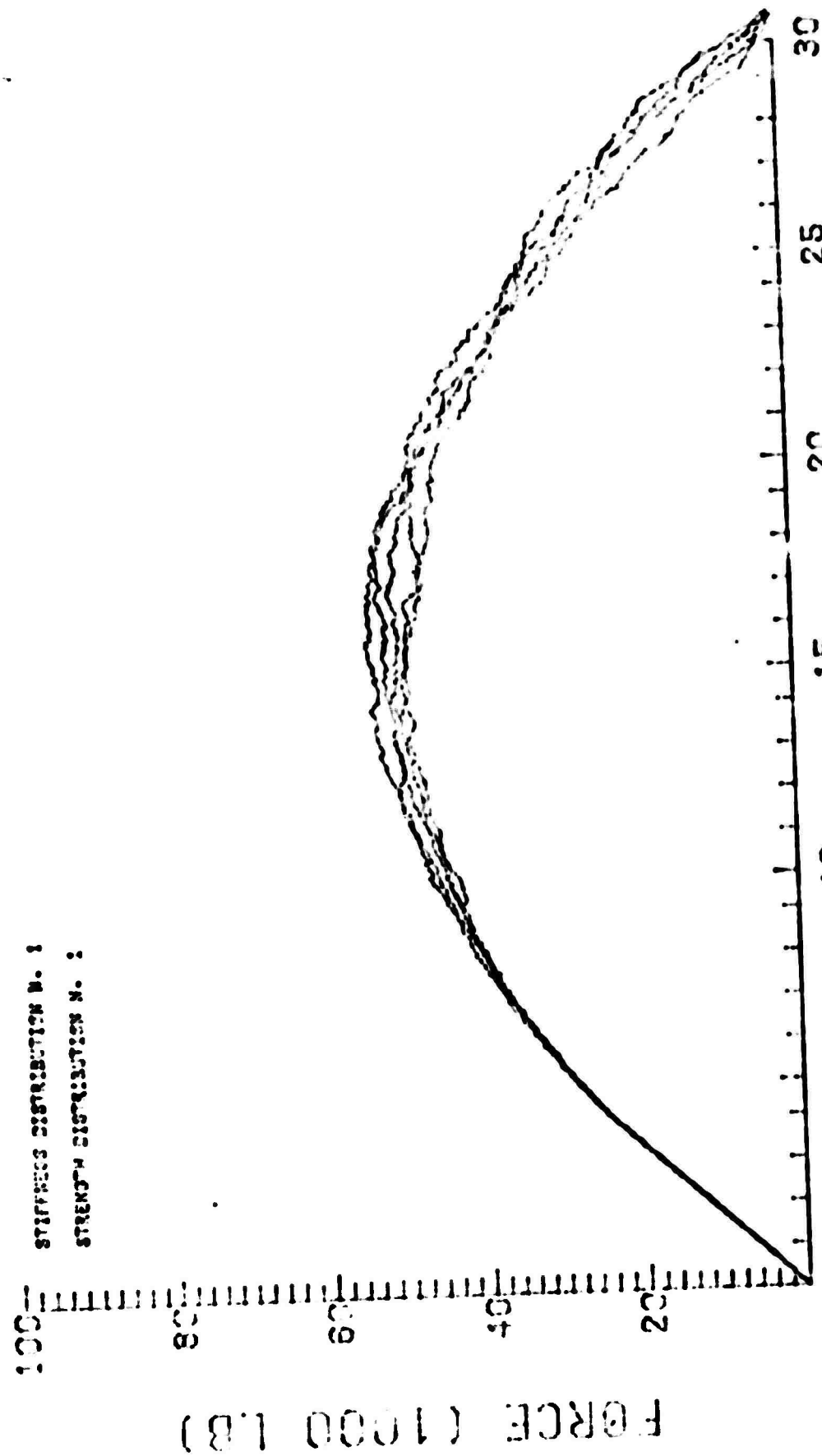

FIGURE I-8 Effect of V_K

FIGURE V-3 Effect of varying stiffness distribution

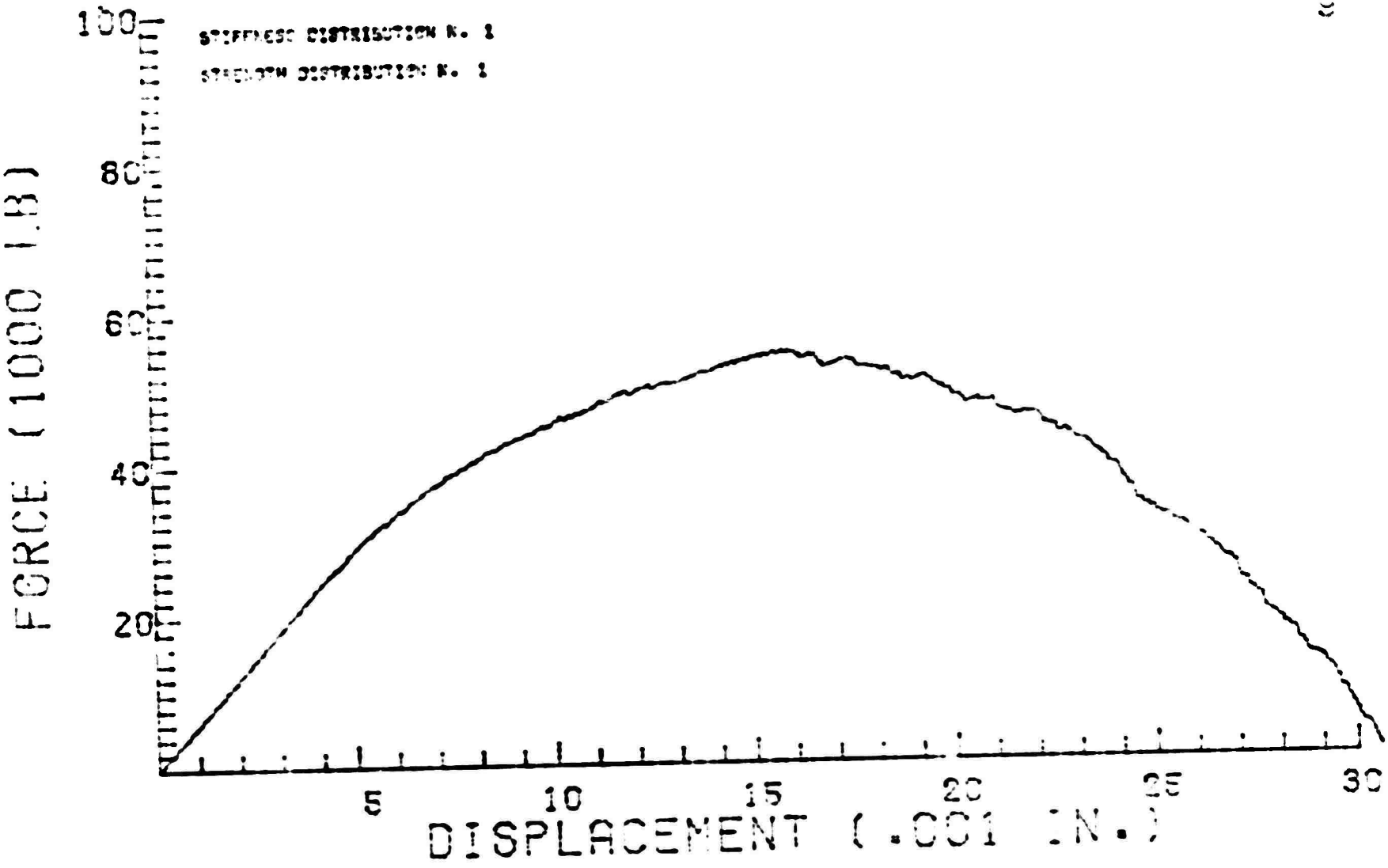

FIGURE II-10 Strength Distribution Uniform

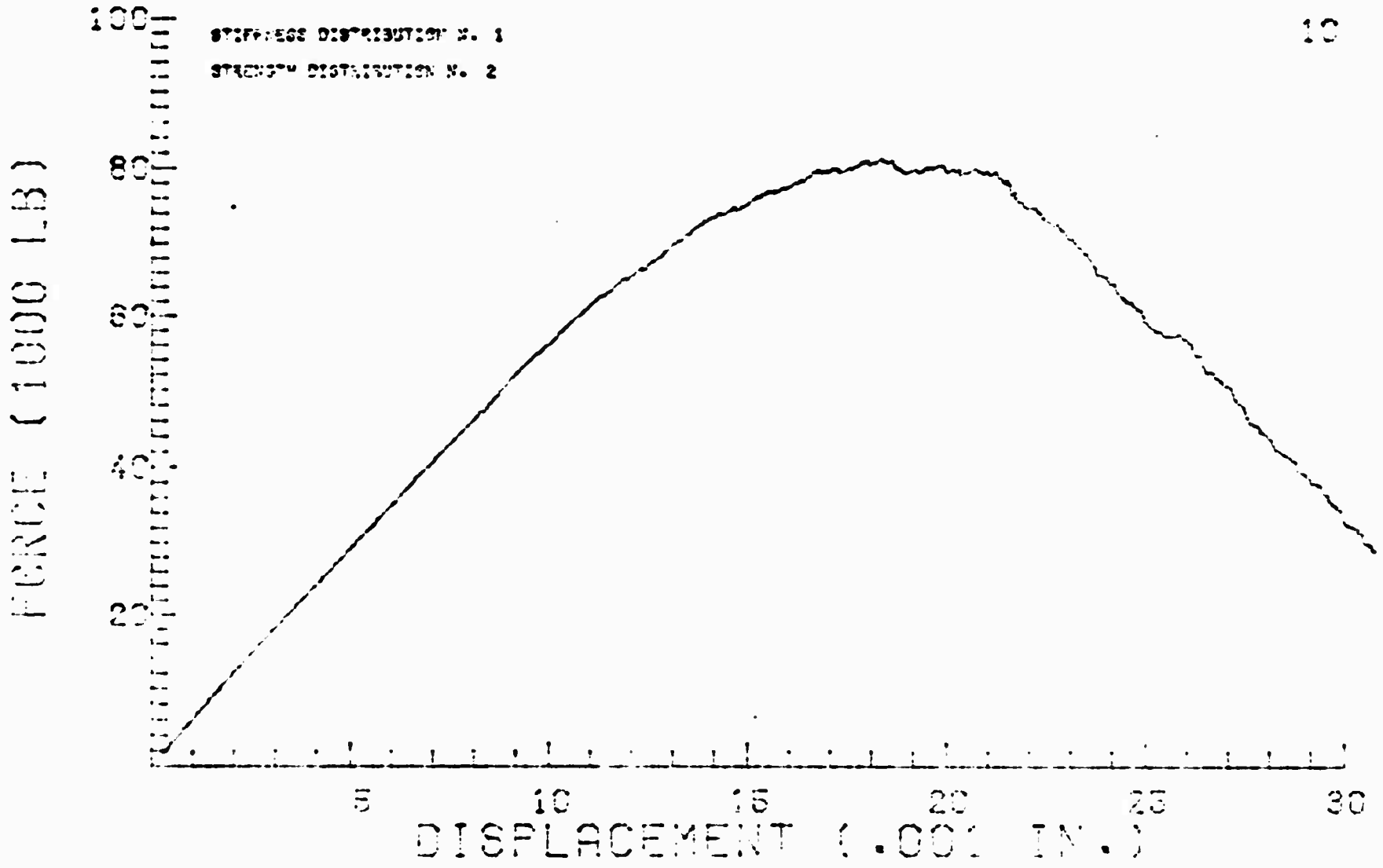

FIGURE II-11 Strength Distribution Unimodal

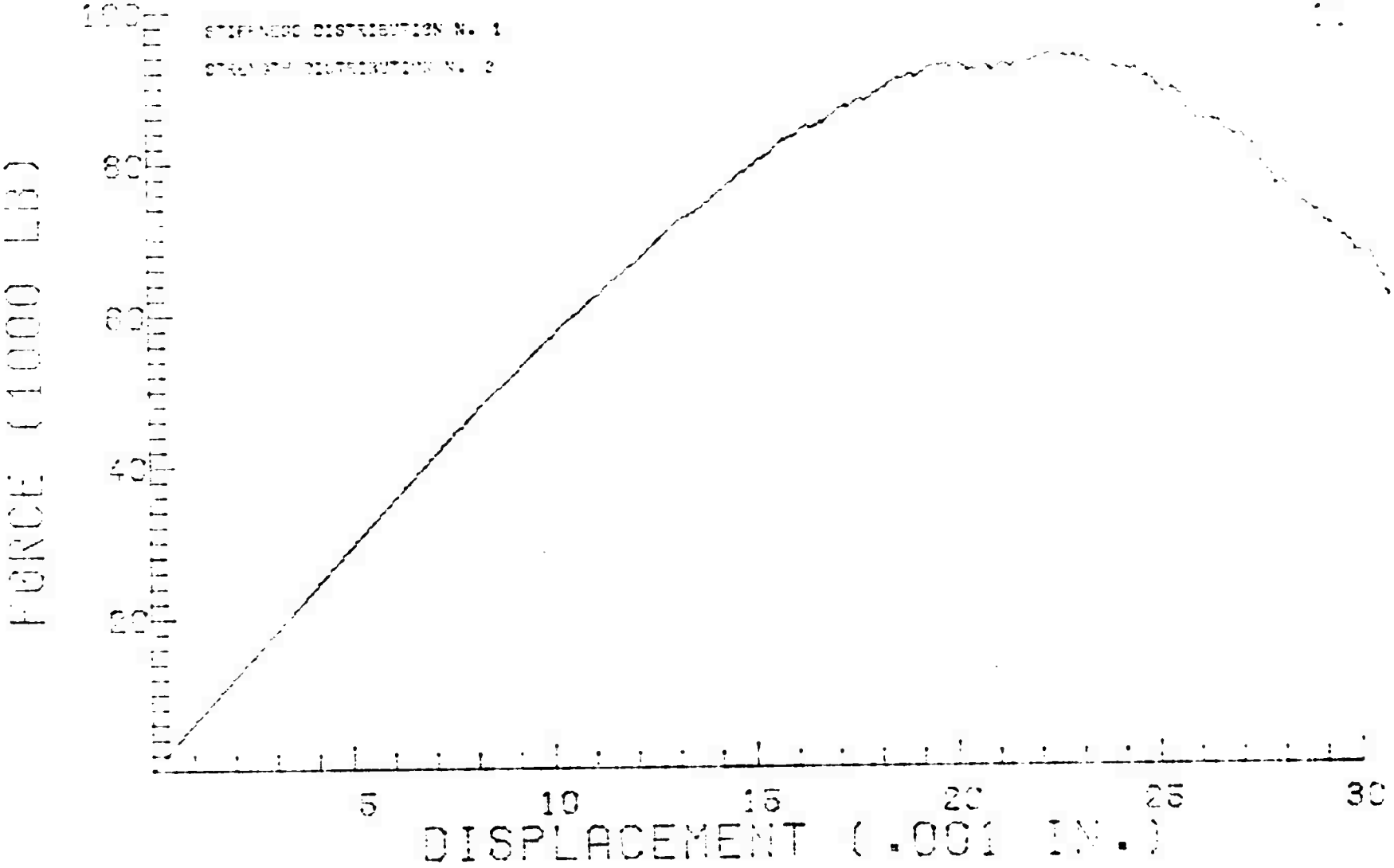

FIGURE II-12 Strength Distribution Left-Skewed

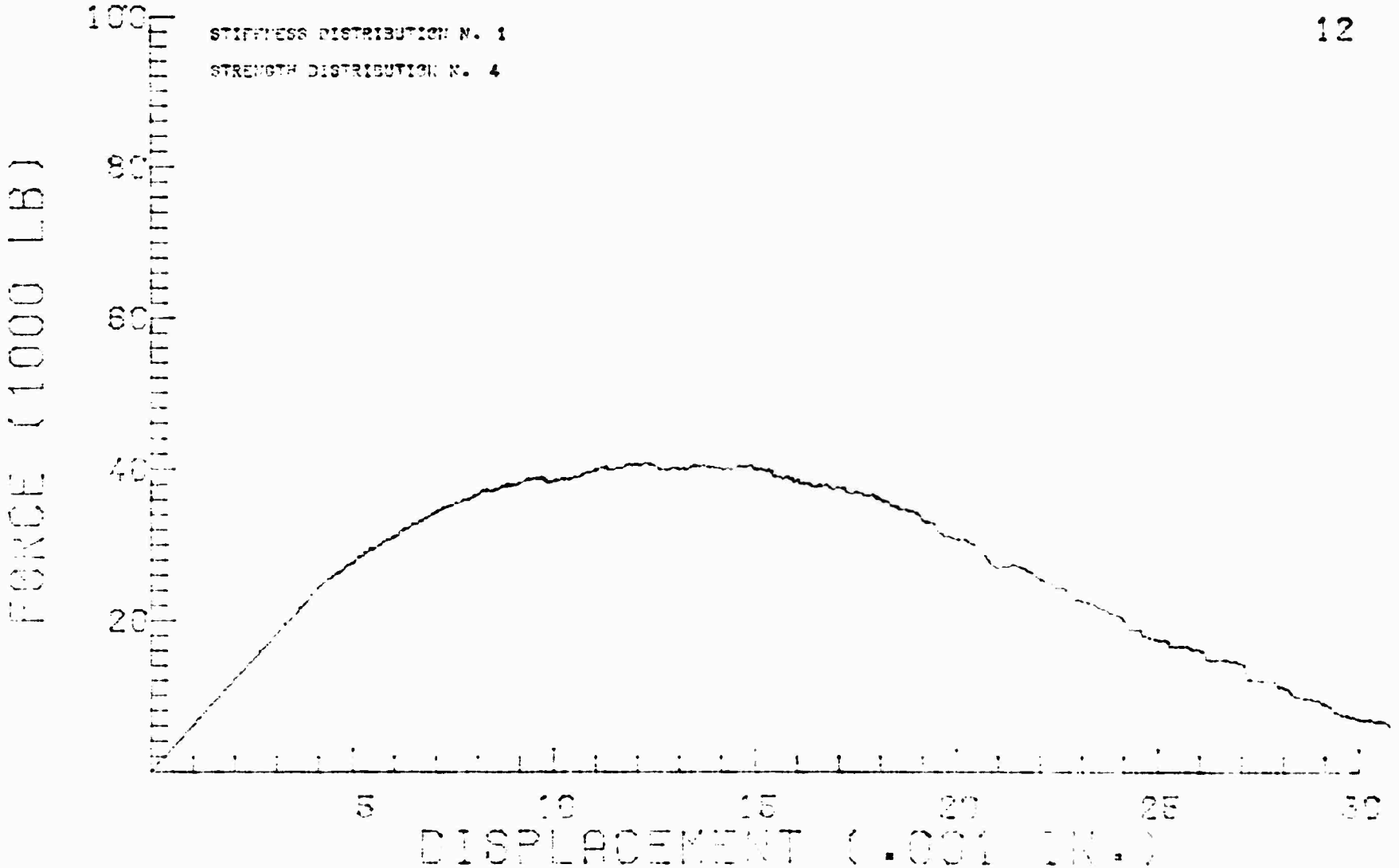

FIGURE II-13 Strength Distribution Right-Skewed

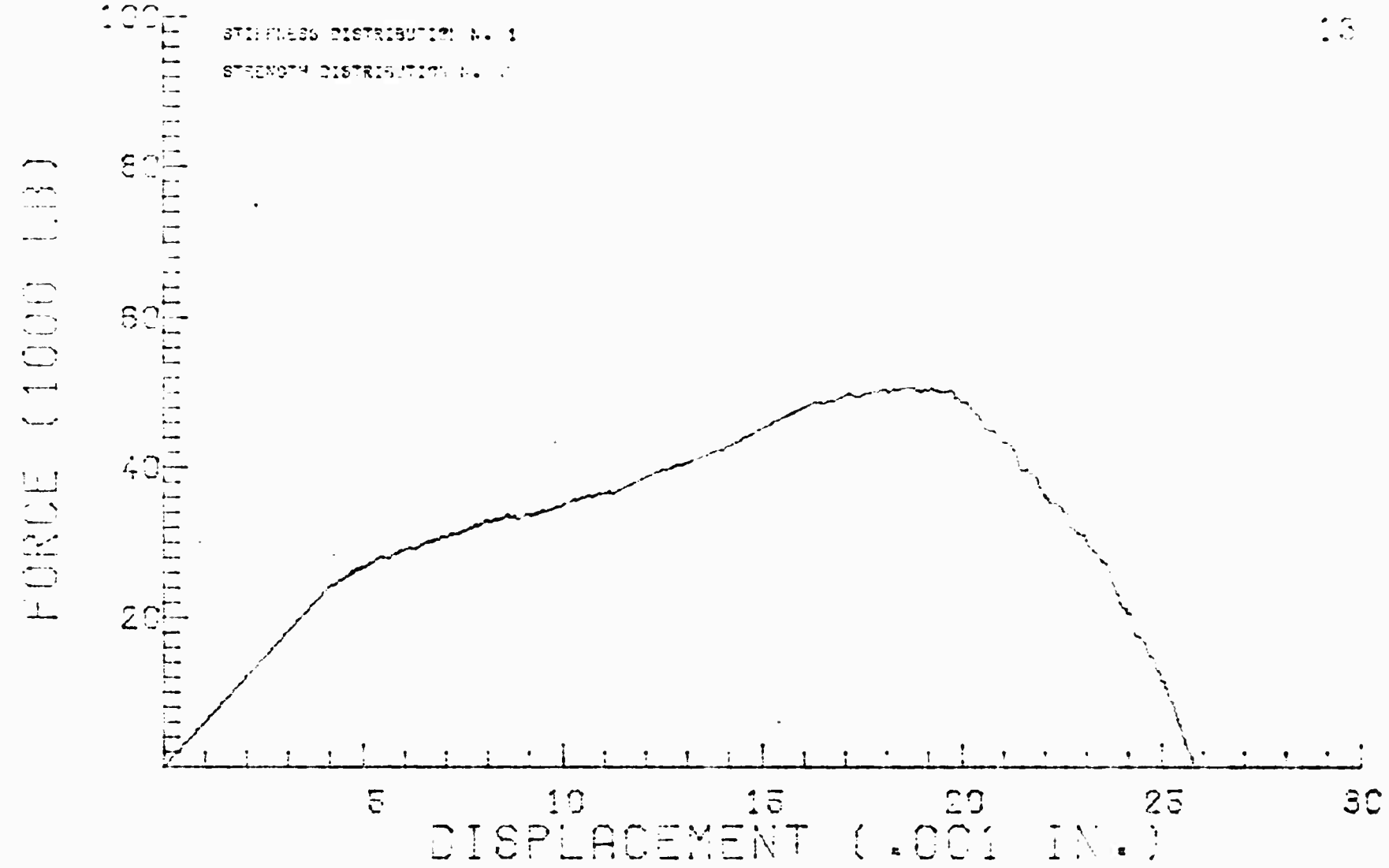

FIGURE II-14 Strength Distribution Bimodal

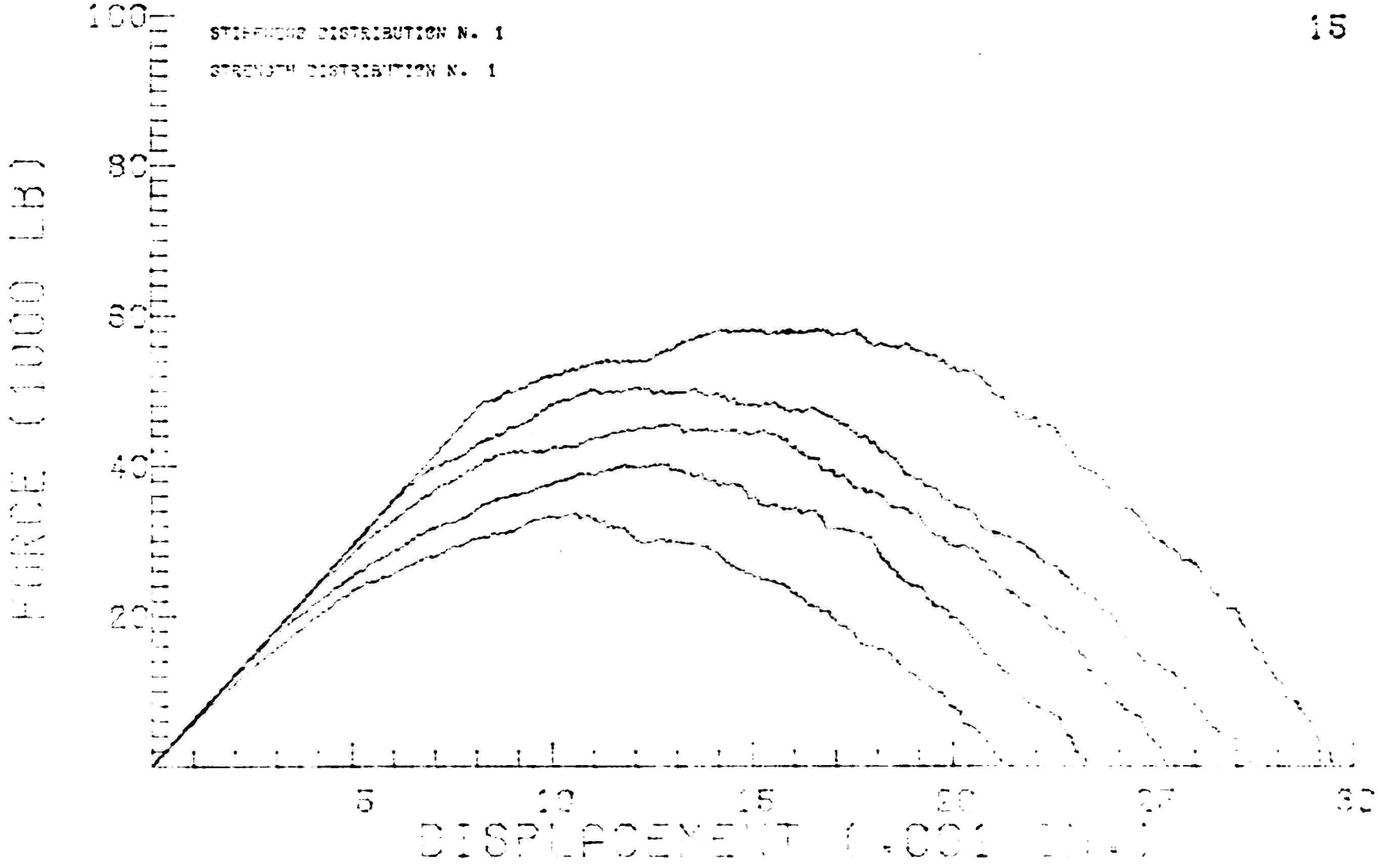

FIGURE II-15 Effect of A_s
A_s = 0.00, .002, .004, .006, .008

Hudson's model used a fixed mean rather than a fixed minimum for the strength distribution. Figs. II-16 through II-20 show that the numerical model produces the characteristic "Hudson" family of curves if the mean is fixed, in this case to 0.015 inch.

Regardless of the varying variance, each family of curves is seen to share a common point. This point is always located at the displacement corresponding to the mean of the strength distribution. For the three symmetrical distributions (uniform, unimodal and bimodal), the force at the shared point is the peak force for the homogeneous (no variance) curve. This is because at the mean strength half of the elements have failed and the stiffness is thus cut in half. Similarly, the skewed curves have shared points at one-third and two-thirds the peak force of the homogeneous curves.

Finally, we see that the curves for the no variance case are all identical. This unrealistic behavior is the only possible result of assuming that rock is uniform and that stresses are uniform in a uniaxial test.

Conclusions

The one-dimensional numerical model agrees qualitatively with Hudson's results if similar assumptions are made. The use of bounded distributions and numerical techniques allows the effect of all variables to be examined in detail. In addition it allows physical interpretations to be placed on parameters as follows:

1) The C in Hudson's model (Eq. II-1) is the Young's modulus of the material.
2) C I is the secant modulus at any displacement.
3) The distribution of stiffness, if independent of strength, has no effect.
4) The minimum of the strength distribution determines the yield point.
5) The maximum of the strength distribution determines where the force displacement curve returns to the axis.

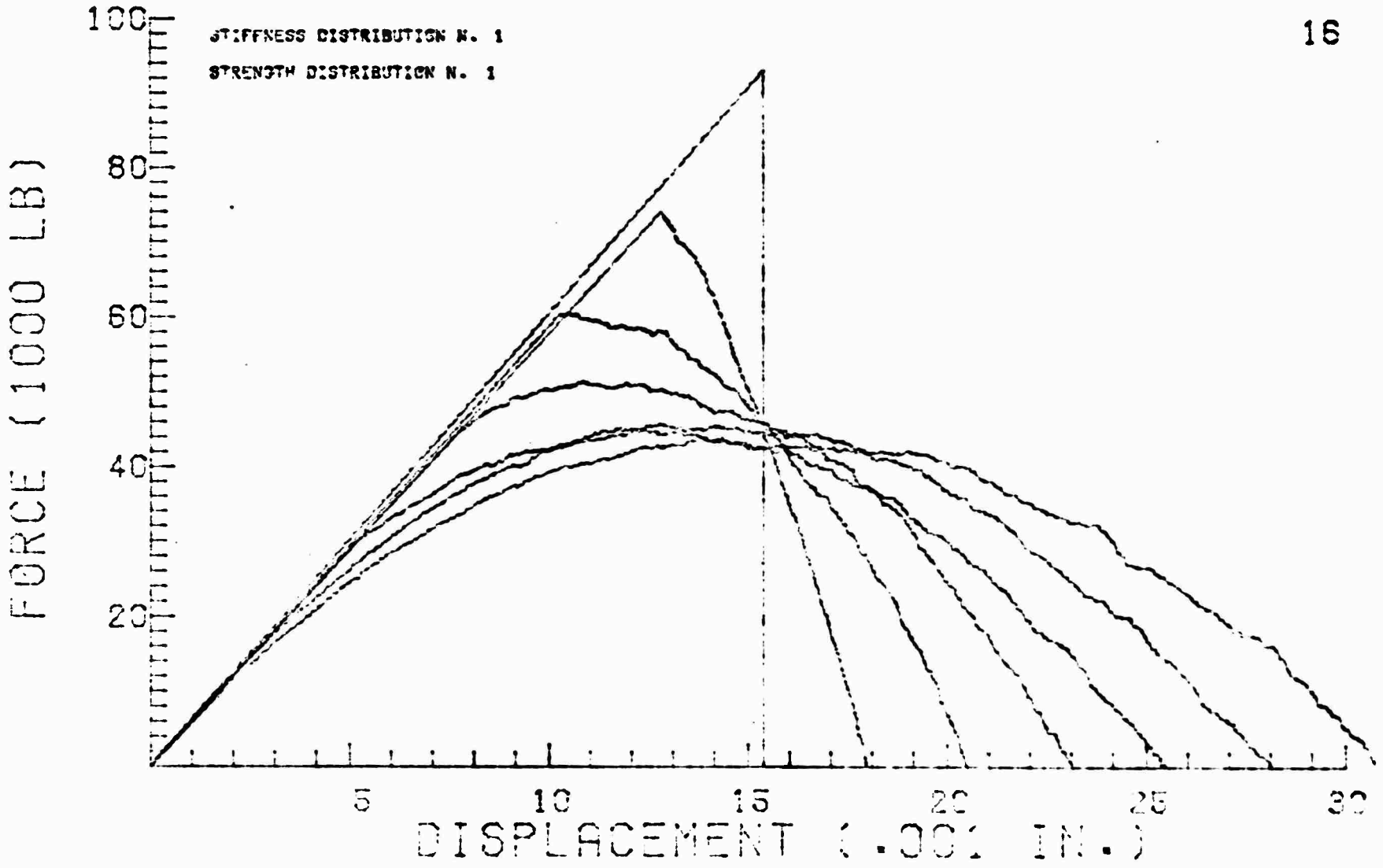

FIGURE II-16 Effect of varying V_s with constant mean strength
Strength Distribution Uniform

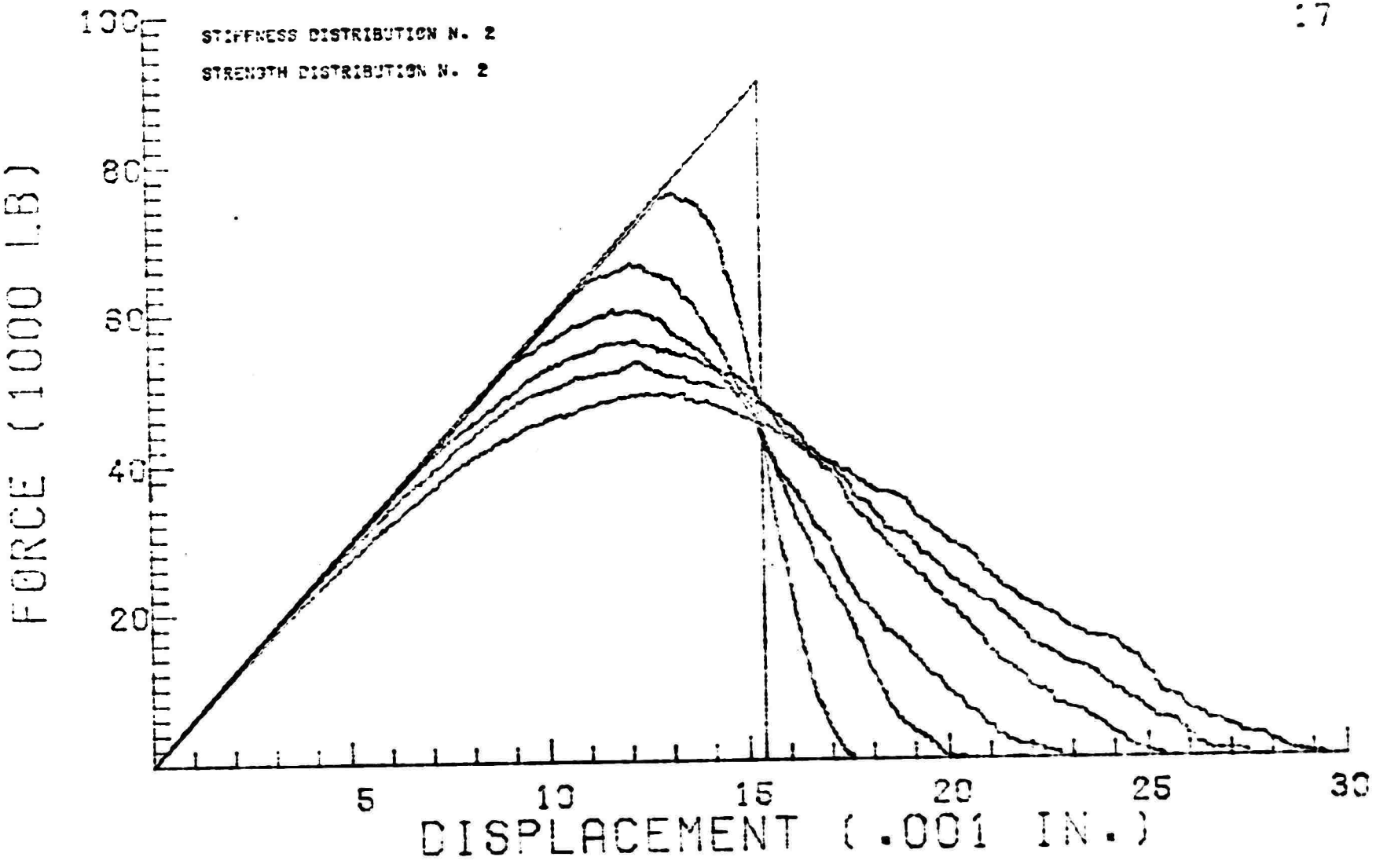

FIGURE II-17 Effect of Varying V_s with Constant Mean Strength Strength Distribution Unimodal

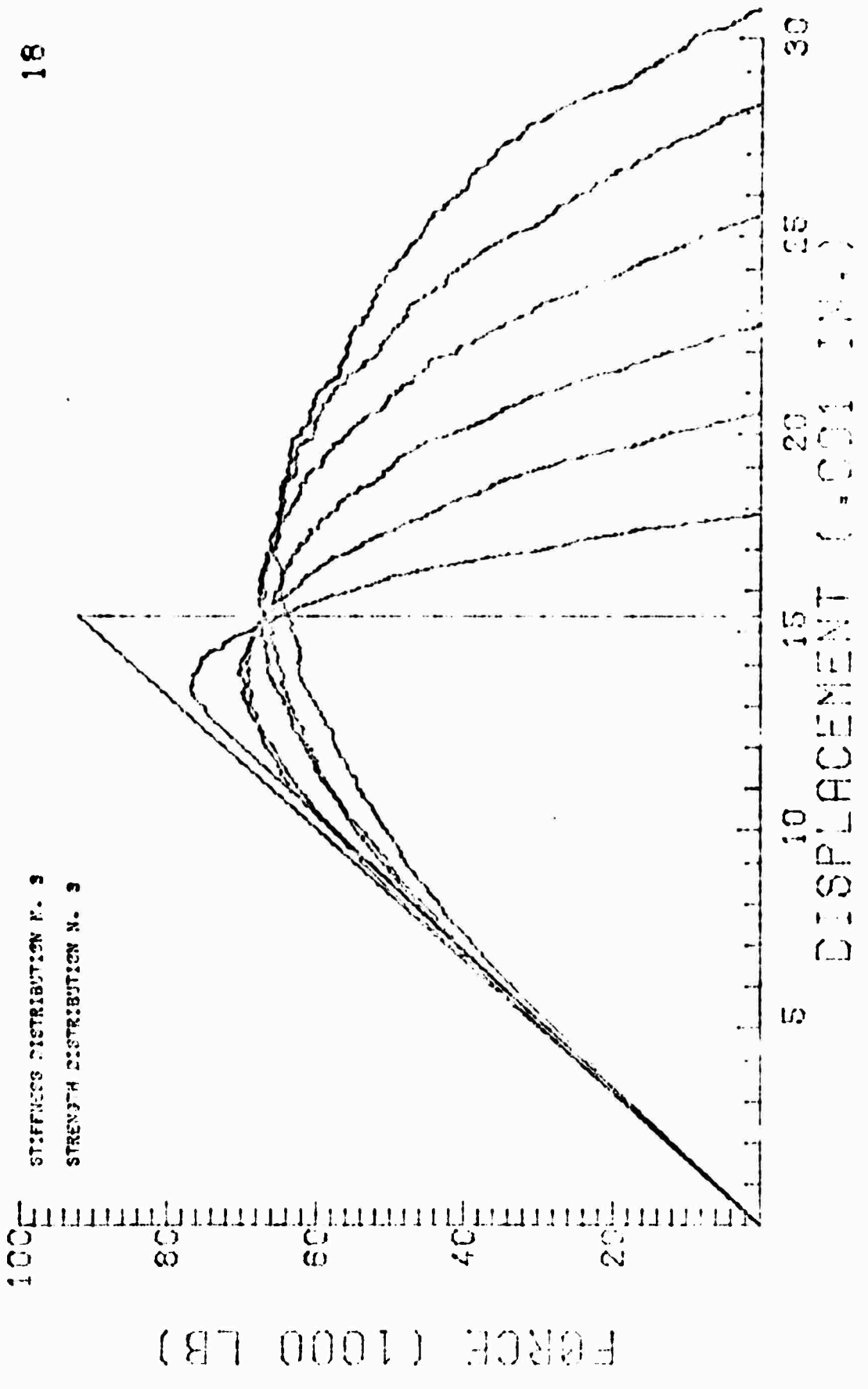

FIGURE II-18 Effect of Varying V_s with Constant Mean Strength
Strength Distribution Left-Skewed

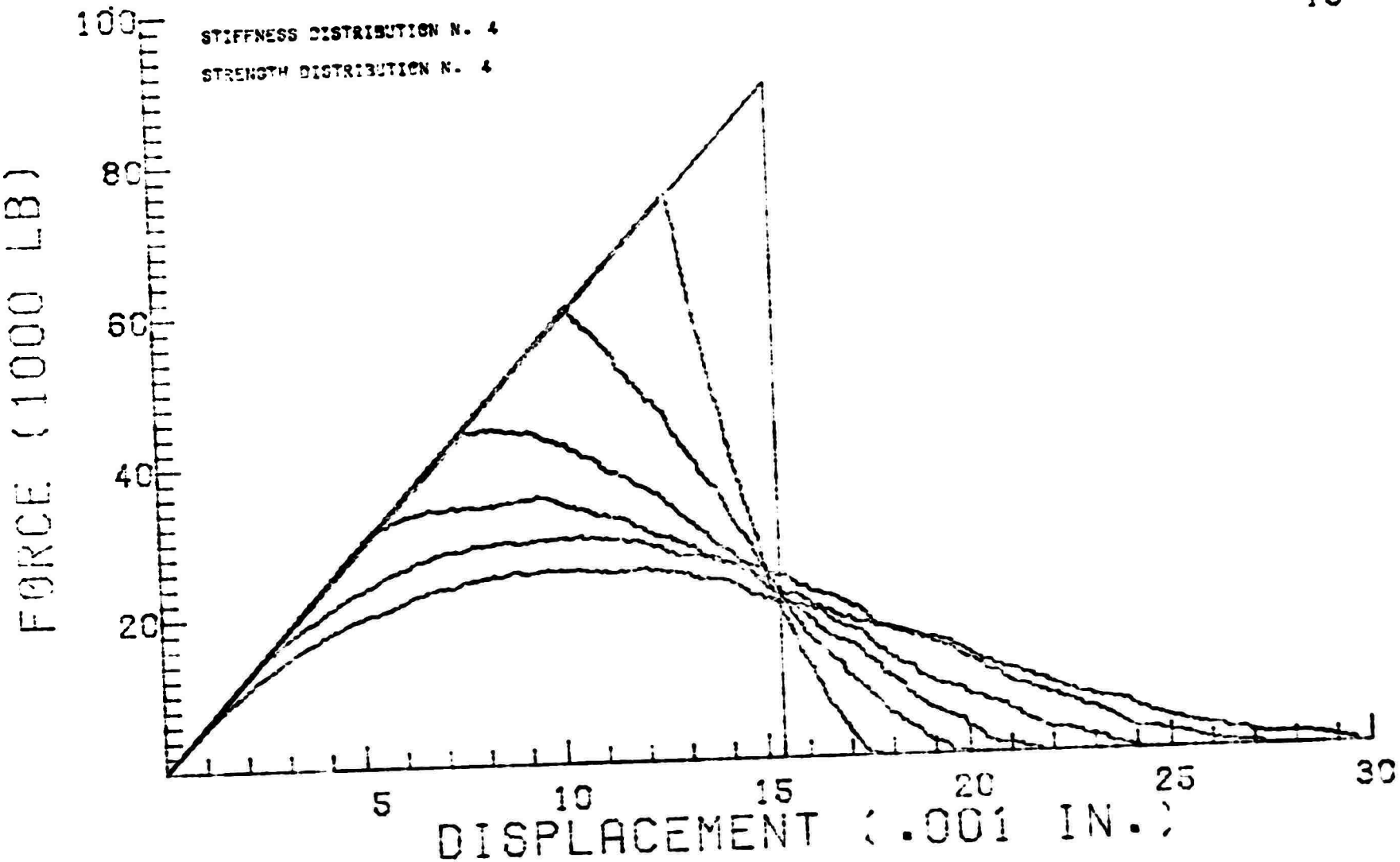

FIGURE II-19 Effect of Varying V_s with Constant Mean Strength
Strength Distribution Right-Skewed

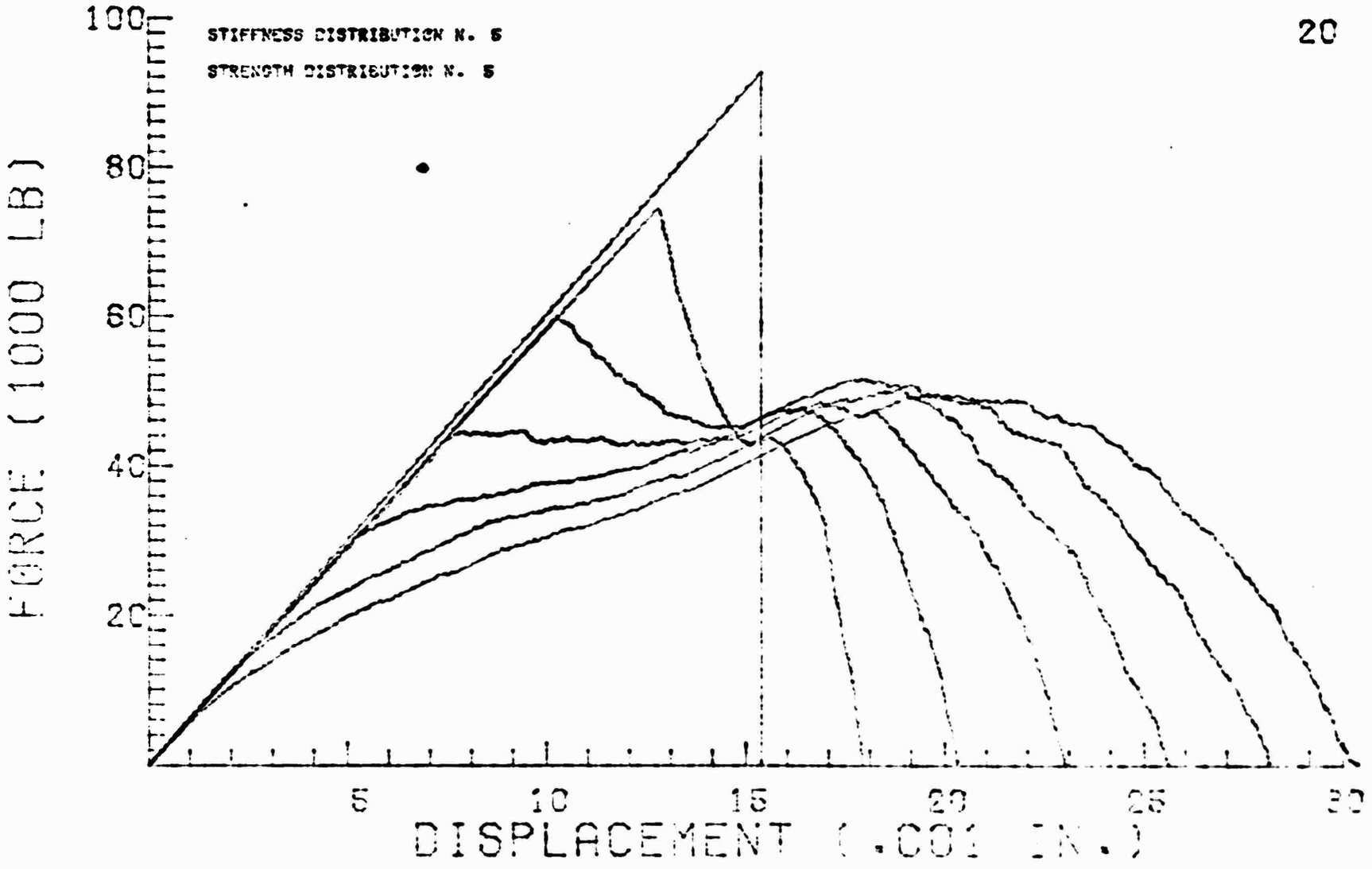

FIGURE II-20 Effect of Varying V_s with Constant Mean Strength
Strength Distribution Bimodal

6) The shape of the force displacement curve can be qualitatively determined in terms of the shape of the strength distribution.

Although it seems unfeasible to quantitatively model a particular rock in a uniaxial test using this method, the model has great value in interpreting the progressive failure of rock in terms of inhomogeneity of the material.

REFERENCES

1. Jaeger, J. C. and N. G. W. Cook. Fundamentals of Rock Mechanics, Methuen, 1969, p. 77.

2. Wawersik, W. R. Detailed Analysis of Rock Failure in Laboratory Compression Tests, Ph. D. Thesis, University of Minnesota, 1968, 165 p.

3. Brown, E. T., J. A. Hudson, M. P. Hardy, and C. Fairhurst. Controlled Failure of Hollow Rock Cylinders in Uniaxial Compression. Rock Mechanics (in press).

4. Hudson, J. A., E. T. Brown, and F. Rummel. The Controlled Failure of Rock Discs and Rings Loaded in Diametral Compression. Submitted to International Journal of Rock Mechanics and Mining Science.

5. Hughes, B. P. and G. P. Chapman, The Complete Stress-Strain Curve for Concrete in Direct Tension, Bulletin RILEM, March 1966, pp. 95-97.

6. Hudson, J. A. Personal communication, 1969.

7. Brown, J. W. and M. M. Singh. An Investigation of Microseismic Activity in Rock Under Tension. Presented at the Annual Meeting of the AIME, New York, Feb. 1966, Preprint No. 66FM31, 30 p.

8. Hudson, J. A. A Critical Examination of Indirect Tensile Strength Tests for Brittle Rocks, Ph. D. Thesis, University of Minnesota, 1970, 161 p.

9. Brown, E. T. Strength-Size Effects in Rock Material, University of Minnesota, Mineral Resources Research Center, Progress Report No. 24, April 1971, pp. 138-150.

10. Weibull, W. A Statistical Theory of the Strength of Materials, Ingeniovs Vetenskaps Akademien Handlingar, No. 151, 1939, pp. 5-44.

11. Weibull, W. The Phenomenon of Rupture in Solids, Ingeniovs Vetenskaps Akademien Handlingar, No. 153, 1939, pp. 5-55.

12. Kececioglu, D. and D. Cormier. Designing a Specified Reliability Directly into a Component, Third Annual Aerospace Reliability and Maintainability Conference, Washington, D. C., June 1964, pp. 546-565.

13. Haugen, E. B. Probabilistic Approaches to Design, Wiley, 1968, 321 p.

14. Hemmerle, W. J. Statistical Computations on a Digital Computer, Blaisdell, 1967, p. 54.

15. University of Wisconsin Computing Center, Random Number Routines, Mathematical Routines Series, UWCC, October 1969, 15 p.

16. Naylor, T. H., J. L. Balintfy, D. S. Burdick, and K. Chu. Computer Simulation Techniques, Wiley, 1966, pp. 70-79.

APPENDIX A
DISTRIBUTIONS

The five distribution functions used in this study are based on a set of functions suggested by Hemmerle (14) for digital computing. The first, the uniform distribution, is well known, and the others are derived from it in the following way:

1) A variate from the unimodal distribution is obtained by adding two random variates from the uniform distribution.
2) A variate from either of the skewed distributions is obtained by doubling either the largest (RSKEW*) or the smallest (LSKEW*) of two variates from the uniform distribution.
3) A variate from the bimodal distribution is obtained taking a variate from the unimodal distribution and subtracting from 1 if less than 1 and from 3 if greater than 1.

Most large computers have available a subroutine which produces pseudo-random uniformly distributed numbers. At UWCC (the University of Wisconsin Computing Center), a function RANUN which can be called from Fortran programs, returns uniform variates in the range 0 to 1 (15). Since the uniform variates are in the range 0 to 1, the procedures described above for the other distributions produce numbers in the range 0 to 2. In order to provide numbers in the range a to b, a scaling technique suggested by Naylor, et al. (16), was used.

To test the generation and scaling routines cumulative distribution functions were found for 1,000 variates in the range 2 to 8 for each distribution. These are shown in Figs. A-1 to A-5 and are seen to match very well the functions expected from integration of the continuous distribution functions.

---

*Subroutine RSKEW actually produces a distribution which is left skewed, i.e., the mean of the distribution is to the right of the midpoint with the tail of the distribution stretched out to the left. Similarly, LSKEW produces a right skewed distribution.

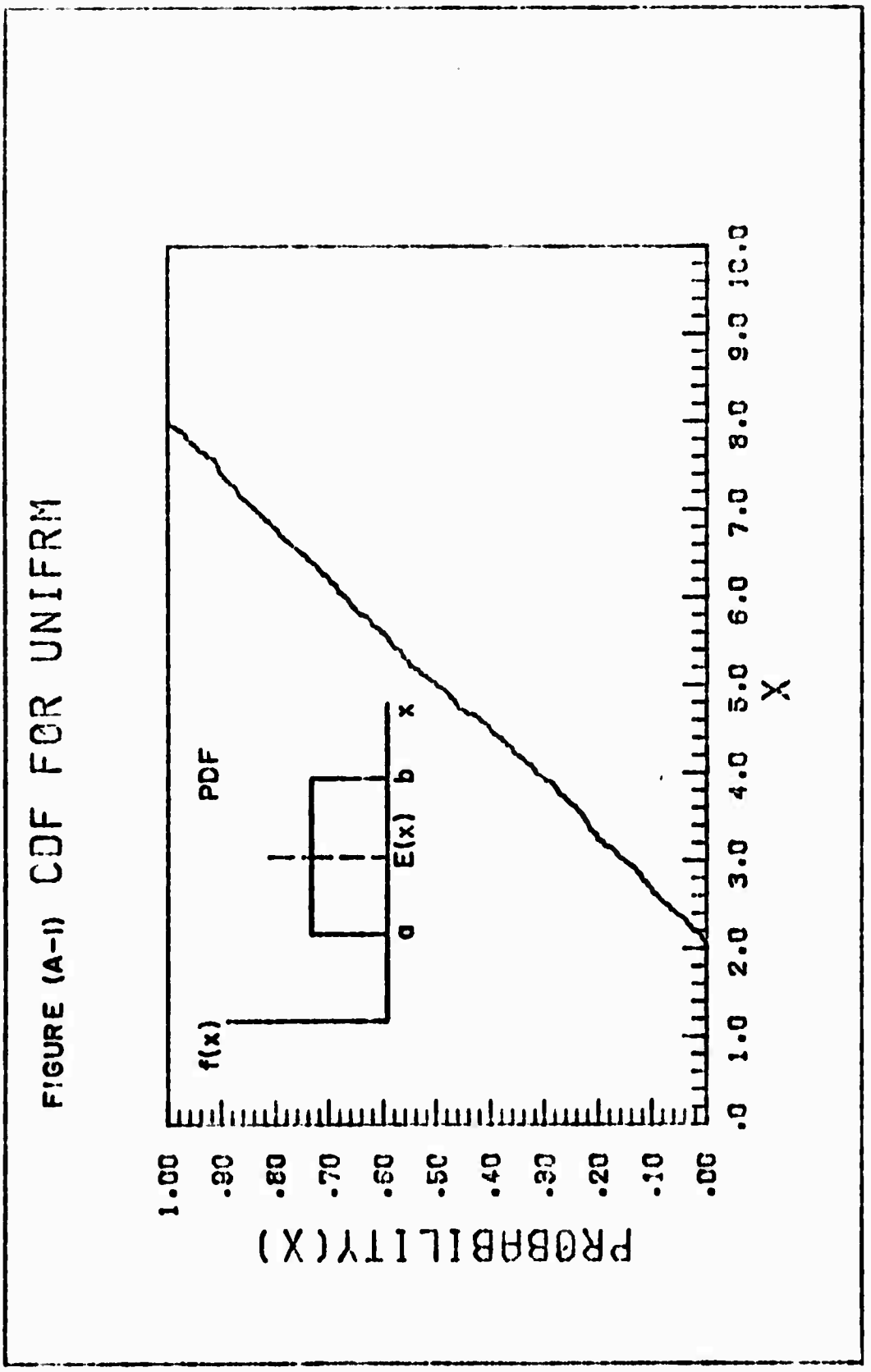
FIGURE (A-1) CDF FOR UNIFRM
PROBABILITY(X)
1.00
.90
.80
.70
.60
.50
.40
.30
.20
.10
.00
.0
1.0
2.0
3.0
4.0
5.0
6.0
7.0
8.0
9.0
10.0
X
PDF
f(x)
a
E(x)
b
x

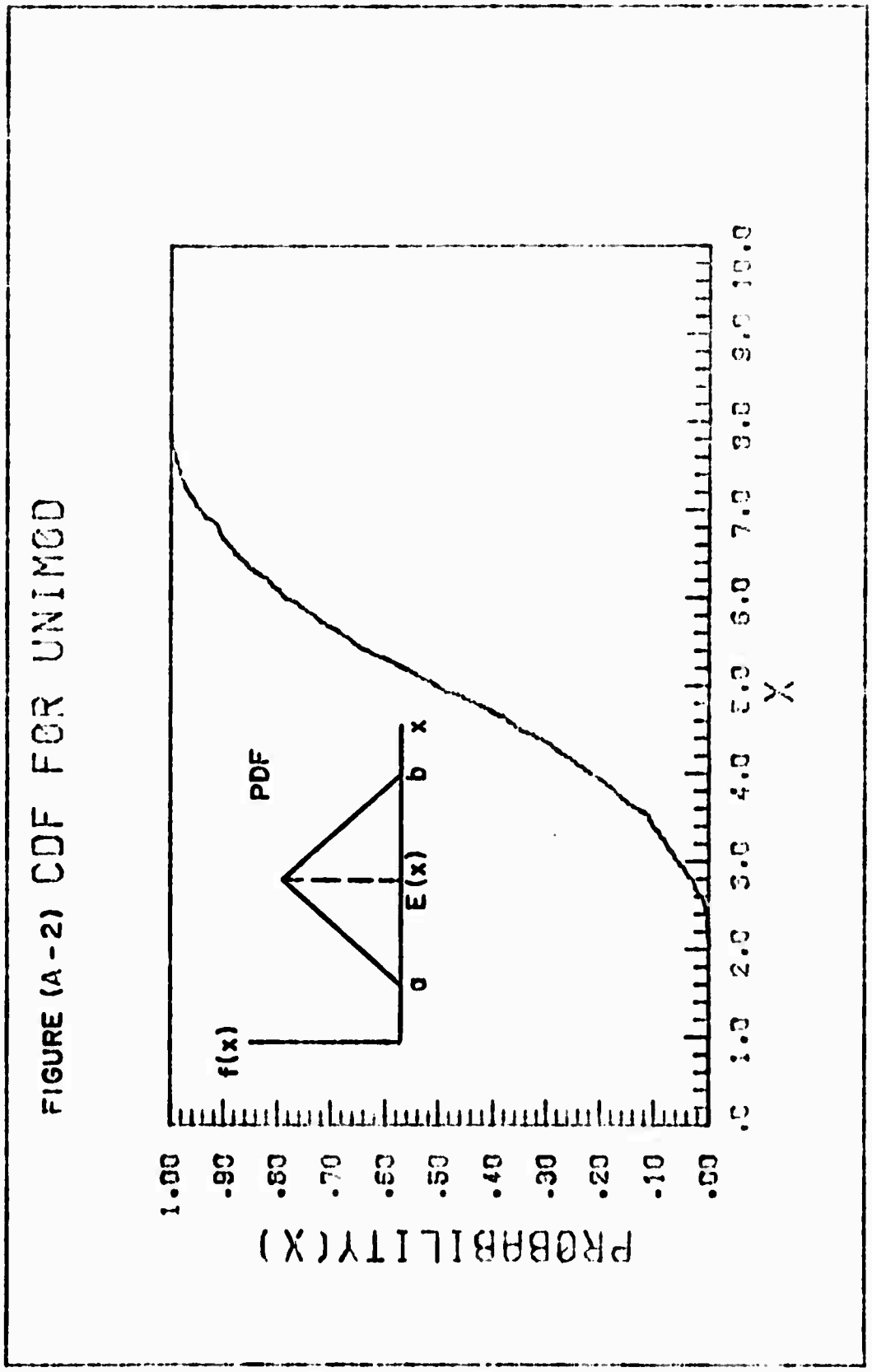

FIGURE (A-2) CDF FOR UNIMOD

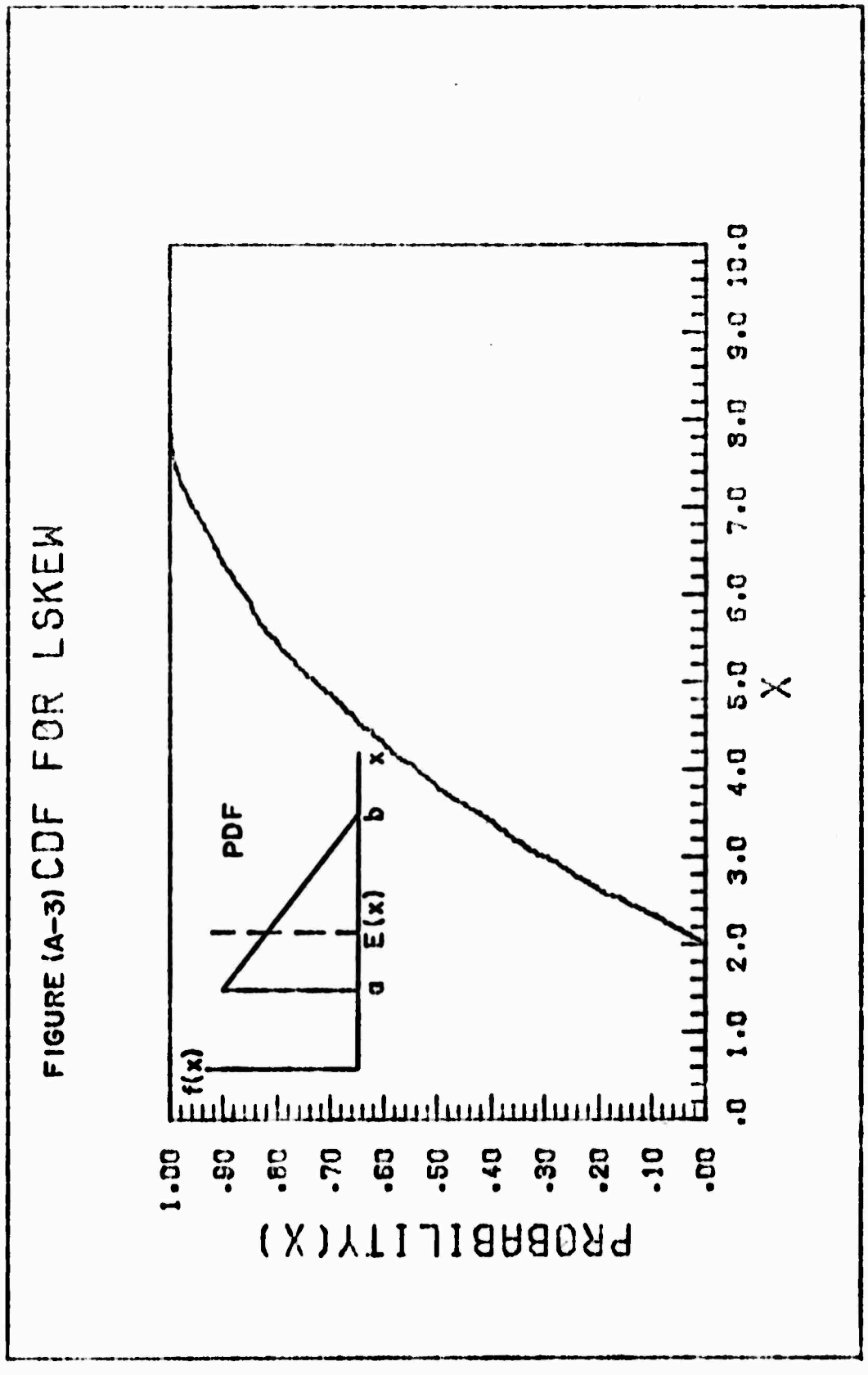

FIGURE (A-3) CDF FOR LSKEW

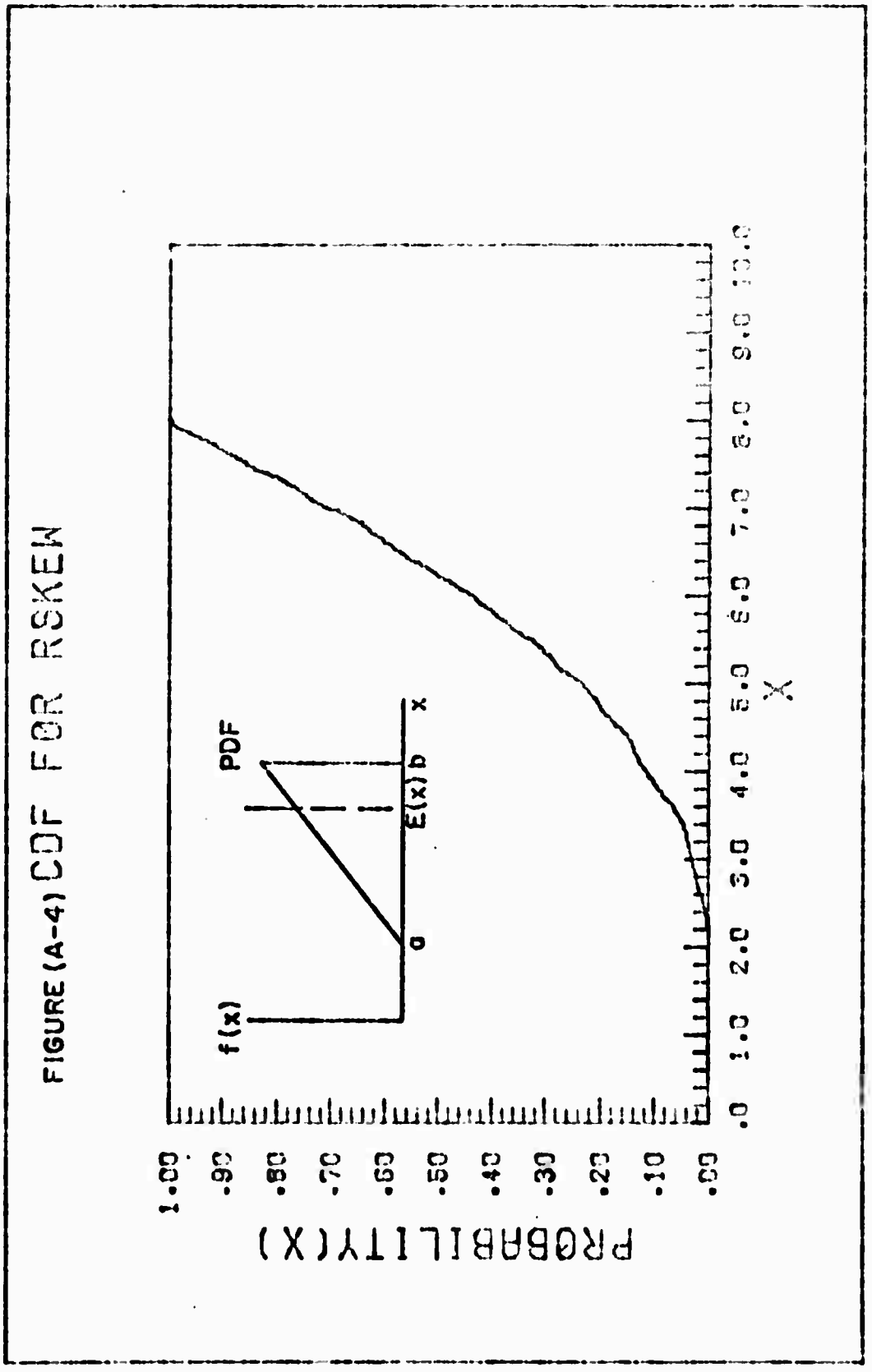

FIGURE (A-4) CDF FOR RSKEW

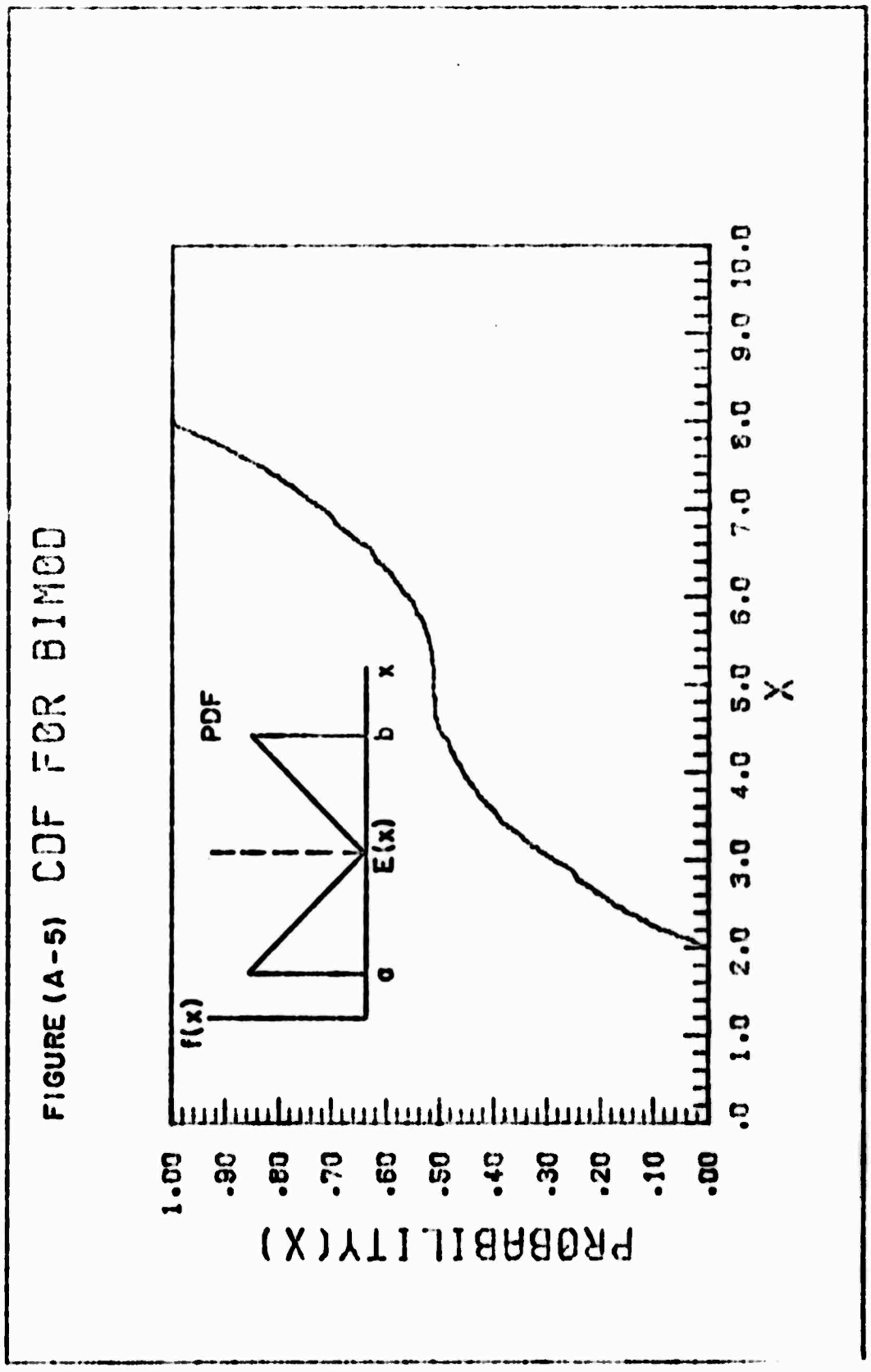

FIGURE (A-5) CDF FOR BIMOD

It should be noted that except for the uniform distribution the functions used are not stochastically derivable (justifiable) in the sense that the normal, gamma, and other commonly used in simulation are. There is no reason whatever to expect that these distributions represent the properties of real rock. (There is, however, nothing which, at the present time at least, would lead to an expectation that any other distribution represents rock properties. This problem is unstudied and relatively unstudiable as well). They were chosen because they are cheap to generate on a digital computer (a single normal variate requires the generation of 12 uniform variates by the Teichroew approximation (16) or from 6 to 12 times longer than methods used here), and because they represent a sufficient variety of behavior that the effect of distribution shapes on progressive failure could be thoroughly examined. An added benefit is that the distributions are all bounded on a range of a to b, allowing physical interpretation to be placed on the bounds a and b.

As proposed by Hemmerle, the statistics of the 4 derived distributions had not been studied, and calculation of the mean and variance were required according to:

$$E(x) = \int_a^b x\, f(x)\, dx \qquad (A\text{-}1)$$

and

$$E(x^2) = \int_a^b x^2\, f(x)\, dx \qquad (A\text{-}2)$$

The results of these integrations are shown in Table A-1. Also shown is the width of each distribution (b-a) in terms of the variance V(X) where V(X) is given by:

$$V(X) = E(x^2) - [E(x)]^2 \qquad (A\text{-}3)$$

TABLE A-1

STATISTICS FOR FIVE DISTRIBUTIONS

No.	Distribution	E(X)	$E(X^2)$	b-a
1	Uniform (UNIFRM)	$\frac{a+b}{2}$	$\frac{a^2+ab+b^2}{3}$	12V
2	Unimodal (UNIMOD)	$\frac{a+b}{2}$	$\frac{7a^2+10ab+7b^2}{24}$	12V
3	Right Skewed (LSKEW)	$\frac{b+2a}{3}$	$\frac{b^2+2ab+3a^2}{6}$	18V
4	Left Skewed	$\frac{2b+a}{3}$	$\frac{3b^2+2ab+a^2}{6}$	18V
5	Bimodal	$\frac{a+b}{2}$	$\frac{3a^2+2ab+3b^2}{8}$	8V

APPENDIX B

ONE-DIMENSIONAL PROGRAM

The following pages contain a listing of the main program and seven subroutines, all in Fortran IV which were used to produce the force-displacement plots in Chapter II. The programs contain references to numerous subroutines provided by the University of Wisconsin Computing Center (UWCC) as system library routines. Most of these are involved with the graphics package which produced the plots. The operation of the programs is described briefly below. While the programs as presented can be run only on the Univac 1108 at UWCC, it is hoped that some insights into the model can be gained from their presentation here. It is further hoped that the distribution subroutines will be useful to others interested in simulation.

The main program first fills arrays containing element stiffness (STIFF) and strength (DISM) with random variables from the appropriate distribution by calls to GENS and GENK. It computes initial total stiffness (TSTF) and uses a UWCC utility routine (URSORT) to sort both arrays in ascending order of strength. In displacement loading, the force (FORCE) at each load increment is computed as the product of current total stiffness and the failure displacement (DISPL). The total stiffness is then reduced by the stiffness of the failed element. The arrays (FORCE and DISPL) are then scaled and plotted.

Subroutines GENK and GENS fill arrays STIFF and DISM, respectively, with random variables by calls to appropriate distribution subroutines. These array-filling routines also compute sample statistics for comparison with distribution statistics.

The distribution subroutines (UNIFRM, UNIMOD, RSKEW, LSKEW, BIMOD) obtain random variates from the five distributions as described in Appendix A.

```
C MAIN PROGRAM..ONE DIM.....
      DIMENSION STIFF(1000),DISM(1000),DISPL(1000),FORCE(1000),
     1XDATA(10),YDATA(10),X(2),Y(2)
      EQUIVALENCE(DISM(1),DISPL(2))
      CALL INITPL(10,10,8)
      X(1)=0.
      X(2)=30.
      Y(1)=0.
      Y(2)=100.
    1 READ 101 N,VS,VS,IS,IS,IPLOT,AS,USER
      IF(N.LE.0.) GO TO 100
      PRINT 102
C FORM STIFFNESS MATRIX .....
      CALL GENK (N,IS,VS,STIFF)
C FORM STRENGTH MATRIX .....
      CALL GENS (N,IS,VS,DISM,AS)
C COMPUTE TOTAL STIFFNESS .....
      TSTF=0.
      DO 2 I=1,N
    2 TSTF=TSTF+STIFF(I)
C SORT IN ASCENDING ORDER OF STRENGTHS .....
      CALL URSORT (1,N,DISM,STIFF,DUM1,0,DUM2)
C DISPLACEMENT LOADING .....
      PRINT 103 USER
      DISPL(1)=0.
      FORCE(1)=0.
      DO 3 I=2,N
      FORCE(I)=TSTF*DISPL(I)
      TSTF=TSTF-STIFF(I-1)
    3 CONTINUE
      CALL URSRCH (0,N,FORCE,L,PEAK,0,DU)
      PRINT 104 L,FORCE(L),DISPL(L),DISPL(N),FORCE(2),DISPL(2)
      DO 6 I=1,N
      DISPL(I)=DISPL(I)*1000.
    6 FORCE(I)=FORCE(I)*0.001
      GO TO (1,4,5),IPLOT
    4 CALL OPLOT (N1,NBLOK,D2,D3,N4)
      CALL PAGE (11.,8.5,0.,6HBORDER)
      CALL SCALE (X,2,XDATA,1.6,5)
      CALL SCALE (Y,2,YDATA,1.10,5)
      CALL BASIS (2.,2.,XDATA,8.,0.,YDATA,5.,90.)
      CALL PLOT (2.,2.,2HUP)
      XMAJ=2.
      DO 10 I=1,6
      DO 15 J=1,4
      XMIN=XMAJ+(J*0.27)
      CALL PLOT(XMIN,2.0,4HDOWN)
      CALL PLVCTR(0.,.1,4HDOWN)
```

```
   15 CALL PLOT (XMIN,2.,2HUP)
      XMAJ=XMAJ+1.3
      CALL PLOT (XMAJ,2.,4HDOWN)
      CALL PLVCTR(0.,0.15,4HDOWN)
      INUM=5*I
      XNUM=XMAJ-0.1
      CALL PLNUMB(XNUM,1.7,INUM,2HI2,0.14,0.)
   10 CALL PLOT (XMAJ,2.,2HUP)
      CALL PLOT(2.,2.,2HUP)
      YMAJ=2.0
      DO 20 I=1,5
      DO 25 J=1,9
      YMIN=YMAJ+(J*0.1)
      CALL PLOT (2.,YMIN,4HDOWN)
      CALL PLVCTR (0.1,0.,4HDOWN)
   25 CALL PLOT (2.,YMIN,2HUP)
      YMAJ=YMAJ+1.
      CALL PLOT (2.,YMAJ,4HDOWN)
      CALL PLVCTR (0.15,0.,4HDOWN)
      INUM=20*I
      YNUM=YMAJ-0.07
      CALL PLNUMB (1.6,YNUM,INUM,2HI2,0.14,0.)
   20 CALL PLOT (2.0,YMAJ,2HUP)
      CALL PLTEXT (1.3,3.,'FORCE (1000 LB)$',0.21,90.)
      CALL PLTEXT (3.75,1.4,'DISPLACEMENT (.001 IN.)$',0.21,0.)
      CALL LINE (DISPL,XDATA,FORCE,YDATA,N,4HNONE,5HSOLID,6HCLOSED)
      CALL PLTEXT(2.40,6.85,'STIFFNESS DISTRIBUTION N.$',.07,0.)
      CALL PLNUMB (4.25,6.85,IK,2HI1,.07,0.)
      CALL PLTEXT(2.4,6.6,'STRENGTH DISTRIBUTION N.$',.07,0.)
      CALL PLNUMB(4.2,6.60,IS,2HI1,.07,0.)
      CALL PLNUMB (9.25,6.85,NSER,2HI4,0.14,0.)
      CALL OPLOT (N1,NBLOK2,D2,D3,N4)
      PRINT 105 NBLOK,NBLOK2
      GO TO 1
    5 CALL LINE (DISPL,XDATA,FORCE,YDATA,N,4HNONE,5HSOLID,6HCLOSED)
      GO TO 1
C FORMAT STATEMENTS ..........................................
  101 FORMAT (I4,2F6.1,3I1,E7.2,I4)
  102 FORMAT(1H1,28X,12F16.8)
  103 FORMAT (1H0,28HDISPLACEMENT LOADING RESULTS,35X,I4)
  104 FORMAT (1H0,14,10X,11HBREAK FORCE=,F7.1,10HBREAK DISP=,F8.4,
     19HMAX DISP=,F8.4//1H ,12HYIELD FORCE=,F7.1,11HYIELD DISP=,F8.4)
  105 FORMAT (1H0,13HBLOCK ADDRESS,3X,I16,3X,2HTO,I16)
  100 CALL ENDPLT
      END
```

```
      SUBROUTINE GENK (N,IK,VK,STIFF)
      DIMENSION STIFF(N)
      CALL RANNUG(NG)
      FK=6000000./N
      SUMX=0.
      SUMX2=0.
      GO TO(1,3,5,7,9),IK
    1 B=FK+SQRT(2.*VK)
      A=2.*FK-B
      DO 2 I=1,N
      CALL UNIFRM (A,B,X)
      SUMX=SUMX+X
      SUMX2=SUMX2+(X*X)
    2 STIFF(I)=X
      GO TO 11
    3 B=FK+SQRT(6.*VK)
      A=2.*FK-B
      DO 4 I=1,N
      CALL UNIMOD(A,B,X)
      SUMX=SUMX+X
      SUMX2=SUMX2+(X*X)
    4 STIFF(I)=X
      GO TO 11
    5 B=FK+SQRT(2.*VK)
      A=3.*FK-2.*B
      DO 6 I=1,N
      CALL RSKEW (A,B,X)
      SUMX=SUMX+X
      SUMX2=SUMX2+(X*X)
    6 STIFF(I)=X
      GO TO 11
    7 B=FK+SQRT(8.*VK)
      A=3.*FK/2.-B/2.
      DO 8 I=1,N
      CALL LSKEW (A,B,X)
      SUMX=SUMX+X
      SUMX2=SUMX2+(X*X)
    8 STIFF(I)=X
      GO TO 11
    9 B=FK+SQRT(2.*VK)
      A=2.*FK-B
      DO 10 I=1,N
      CALL BIMOD (A,B,X)
      SUMX=SUMX+X
      SUMX2=SUMX2+(X*X)
   10 STIFF(I)=X
   11 PRINT 101
      XBAR=SUMX/N
```

```
      VARX=(SUMX2/N)-(XBAR*XBAR)
      GO TO (12,13,14,15,16),IK
   12 PRINT 102
      GO TO 17
   13 PRINT 103
      GO TO 17
   14 PRINT 104
      GO TO 17
   15 PRINT 105
      GO TO 17
   16 PRINT 106
   17 PRINT 107,A,B,NG
      PRINT 108,EX,VK
      PRINT 109,XBAR,VARX
  101 FORMAT(1H ,16(6H******)/23H STIFFNESS DISTRIBUTION)
  102 FORMAT(1H+,24X,7HUNIFORM)
  103 FORMAT(1H+,24X,8HUNIMODAL)
  104 FORMAT(1H+,24X,12HRIGHT SKEWED)
  105 FORMAT(1H+,24X,11HLEFT SKEWED)
  106 FORMAT(1H+,24X,7HBIMODAL)
  107 FORMAT(24HODISTRIBUTION RANGE FROM,1PE16.5,3H TO,1PE16.8,
     140X,1PE16.8)
  108 FORMAT(18HODISTRIBUTION MEAN,1PE16.6,8X,8HVARIANCE,1PE16.8)
  109 FORMAT (18HO THIS SAMPLE MEAN,1PE16.8,3X,9HVARIANCE,1PE16.8)
      RETURN
      END
```

```
      SUBROUTINE GENS (N,IS,VS,STRNTH,A)
      DIMENSION STRNTH(N)
      SUMX=0.
      SUMX2=0.
      GO TO(1,3,5,7,9),IS
    1 B=A+SQRT(12.*VS)
      ES=(A+B)/2.
      DO 2 I=1,N
      CALL UNIFRM(A,B,X)
      SUMX=SUMX+X
      SUMX2=SUMX2+(X*X)
    2 STRNTH(I)=X
      GO TO 11
    3 B=A+SQRT(24.*VS)
      ES=(A+B)/2.
      DO 4 I=1,N
      CALL UNIMOD(A,B,X)
      SUMX=SUMX+X
      SUMX2=SUMX2+(X*X)
    4 STRNTH(I)=X
      GO TO 11
    5 B=A+SQRT(18.*VS)
      ES=(2.*B+A)/3.
      DO 6 I=1,N
      CALL RSKEW (A,B,X)
      SUMX=SUMX+X
      SUMX2=SUMX2+(X*X)
    6 STRNTH(I)=X
      GO TO 11
    7 B=A+SQRT(18.*VS)
      ES=(2.*A+B)/3.
      DO 8 I=1,N
      CALL LSKEW (A,B,X)
      SUMX=SUMX+X
      SUMX2=SUMX2+(X*X)
    8 STRNTH(I)=X
      GO TO 11
    9 B=A+SQRT( 9.*VS)
      ES=(A+B)/2.
      DO 10 I=1,N
      CALL BIMOD (A,B,X)
      SUMX=SUMX+X
      SUMX2=SUMX2+(X*X)
   10 STRNTH(I)=X
   11 XBAR=SUMX/N
      VARX=(SUMX2/N)-(XBAR*XBAR)
      PRINT 101
      GO TO (12,13,14,15,16),IS
```

```
   12 PRINT 102
      GO TO 17
   13 PRINT 103
      GO TO 17
   14 PRINT 104
      GO TO 17
   15 PRINT 105
      GO TO 17
   16 PRINT 106
   17 PRINT 107,A,B
      PRINT 108,ES,VS
      PRINT 109,XBAR,VARX
  101 FORMAT(22H0SKEWNESS DISTRIBUTION)
  102 FORMAT(1H+,24X,7HNORMAL)
  103 FORMAT(1H+,24X,8HUNIMODAL)
  104 FORMAT(1H+,24X,12HRIGHT SKEWED)
  105 FORMAT(1H+,24X,11HLEFT SKEWED)
  106 FORMAT(1H+,24X,7HBIMODAL)
  107 FORMAT(24H0DISTRIBUTION RANGE FROM,1PE16.3,3H TO,1PE16.3)
  108 FORMAT(18H0DISTRIBUTION MEAN,1PE16.3,5X,9HVARIANCE,1PE16.3)
  109 FORMAT (18H0 THIS SAMPLE MEAN,1PE16.3,5X,9HVARIANCE,1PE16.3)
      RETURN
      END
```

```
      SUBROUTINE UNIFRV(A,B,X)
      R=RANUN(R)
      X=A+(B-A)*R
      RETURN
      END


      SUBROUTINE UNIMOD(A,B,X)
      R1=RANUN(R)
      R2=RANUN(R)
      X=0.5*(A+B+(B-A)*(R1+R2-1.))
      RETURN
      END


      SUBROUTINE RSKEW(A,B,X)
      R1=RANUN(R)
      R2=RANUN(R)
      IF(R1.GE.R2) GO TO 1
      R=(2.*R2)-1.
      GO TO 2
    1 R=(2.*R1)-1.
    2 X=0.5*(A+B+(B-A)*R)
      RETURN
      END


      SUBROUTINE LSKEW(A,B,X)
      R1=RANUN(R)
      R2=RANUN(R)
      IF(R1.GE.R2) GO TO 1
      R=(2.*R1)-1.
      GO TO 2
    1 R=(2.*R2)-1.
    2 X=0.5*(A+B+(B-A)*R)
      RETURN
      END


      SUBROUTINE RIMOD(A,B,X)
      R1=RANUN(R)
      R2=RANUN(R)
      R=R1+R2-1.
      IF(R.GE.0.) GO TO 1
      R=-(1.+R)
      GO TO 2
    1 R=1.-R
    2 X=0.5*(A+B+(B-A)*R)
      RETURN
      END
```

PART B

MECHANICAL BEHAVIOR OF ROCK UNDER CYCLIC FATIGUE

By Bezalel C. Haimson[1] and Chin Man Kim[2]

INTRODUCTION

Rock and rock structures such as open-pit benches, mine escavations, bridge abutments, dam and road foundations undergo cyclic loading caused by earthquakes, traffic, drilling, blasting, etc. This type of loading often causes a material to fail at a stress lower than its determined strength, a phenomenon called fatigue. Fatigue characteristics are usually presented in the form of an S-N curve (stress level versus the number of cycles required to bring about failure). The top stress value that appears to be unaffected by cyclic loading is sometimes called the fatigue limit. Cyclic fatigue in structural materials such as metals, concrete and soil has been thoroughly investigated in the last decades. Rock fatigue, however, has received only little attention. An early attempt to establish fatigue characteristics of a limestone was inconclusive mainly due to a very limited number of tests undertaken (3). Burdine (1), however, ran an extensive series of compressive cyclic loading tests in Berea Sandstone, discovered that the rock was definitely weakened by repetitive loading, and determined S-N curves for different testing conditions. Hardy and Chugh (4) used modern equipment to improve testing

[1] Assistant Professor, Department of Metallurgical and Mineral Engineering, University of Wisconsin, Madison.

[2] Graduate Student, Department of Metallurgical and Mineral Engineering, University of Wisconsin, Madison.

PART B

MECHANICAL BEHAVIOR OF ROCK UNDER CYCLIC FATIGUE

By Bezalel C. Haimson[1] and Chin Man Kim[2]

INTRODUCTION

Rock and rock structures such as open-pit benches, mine escavations, bridge abutments, dam and road foundations undergo cyclic loading caused by earthquakes, traffic, drilling, blasting, etc. This type of loading often causes a material to fail at a stress lower than its determined strength, a phenomenon called fatigue. Fatigue characteristics are usually presented in the form of an S-N curve (stress level versus the number of cycles required to bring about failure). The top stress value that appears to be unaffected by cyclic loading is sometimes called the fatigue limit. Cyclic fatigue in structural materials such as metals, concrete and soil has been thoroughly investigated in the last decades. Rock fatigue, however, has received only little attention. An early attempt to establish fatigue characteristics of a limestone was inconclusive mainly due to a very limited number of tests undertaken (3). Burdine (1), however, ran an extensive series of compressive cyclic loading tests in Berea Sandstone, discovered that the rock was definitely weakened by repetitive loading, and determined S-N curves for different testing conditions. Hardy and Chugh (4) used modern equipment to improve testing

[1] Assistant Professor, Department of Metallurgical and Mineral Engineering, University of Wisconsin, Madison.

[2] Graduate Student, Department of Metallurgical and Mineral Engineering, University of Wisconsin, Madison.

procedures and concluded that three additional rock types were fatigue prone even under a low maximum number of cycles per test (10,000). The present paper reports the results of the first phase in a comprehensive experimental study of rock cyclic fatigue. The main objectives of the investigation are to provide engineers quantitative results in the form of S-N curves obtained for different rock types under various stress conditions, to determine the fatigue strength of failed rock for the use of mine designers and earthquake researchers, and to provide a better understanding of the fatigue mechanism by strain measurements and careful observations of fabric changes.

LABORATORY EQUIPMENT AND TEST PROCEDURES

Rock Specimens

Two rock types have been used in the reported study. White Tennessee Marble was chosen because of its uniformity, isotropy and fine grain size. It has been extensively tested and is known to have very consistent mechanical behavior (6). Georgia Marble was selected for the ease with which it can be controlled in its post failure mode (the descending part of the complete stress-strain curve).

Cylindrical specimens, 1.0 inch in diameter and 2.5 inch long, were cored out of a large rock block by diamond drilling in one direction only. The automatically-fed coring yielded straight smooth rock cylinders that did not require further machining. Specimen ends were surface ground until flat and parallel faces were obtained to within 0.001 inch. The specimens were then oven dried at 120°F for a week prior to testing.

Apparatus

Specimens were loaded in an electro-hydraulic servo-controlled

loading machine of 100,000 lbs. capacity. A general view of the entire apparatus is shown in Fig. 1. The machine can be programmed

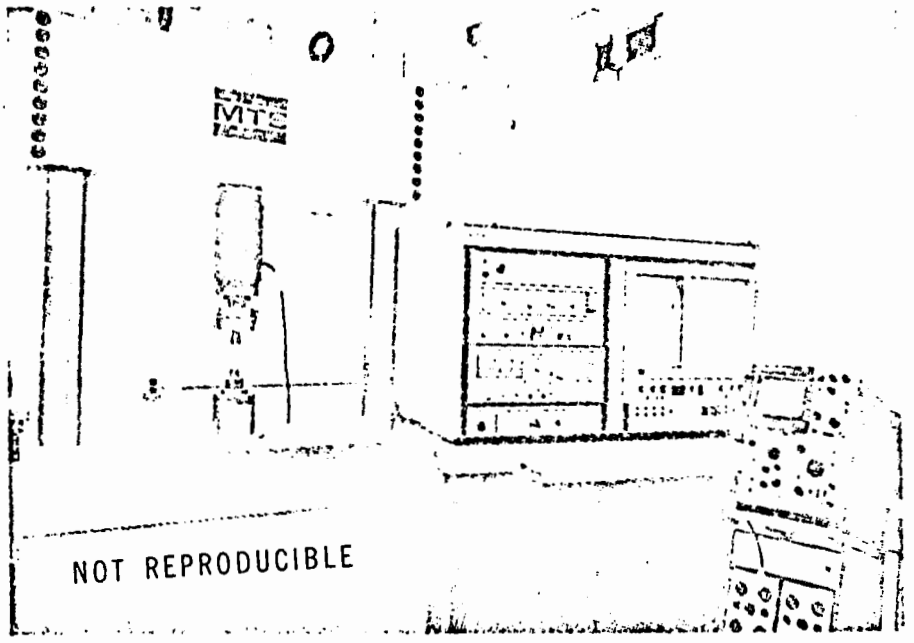

FIG. 1 LOADING SYSTEM, ELECTRONIC CONTROLS AND DATA ACQUISITION INSTRUMENTS.

through a function generator to apply cyclic loading to a specimen by controlling either stress or strain rates. In the experiments described a constant rate of compressive load was applied to specimens using a triangular wave shape. A digital counter gave the number of cycles per test, and an X-Y recorder was used to plot stress-strain or strain-time curves. The load applied to specimens was sensed by a dynamic load cell mounted on the bottom part of the machine crosshead. The longitudinal strain was measured through strain gages mounted on a system of double cantilevers (Fig. 2). The rings holding the cantilever device were threaded on to the platens in contact with the rock specimens and held in place by locking nuts. This method of attachment proved superior to the previously used set-screws which tended to slip in long duration tests.

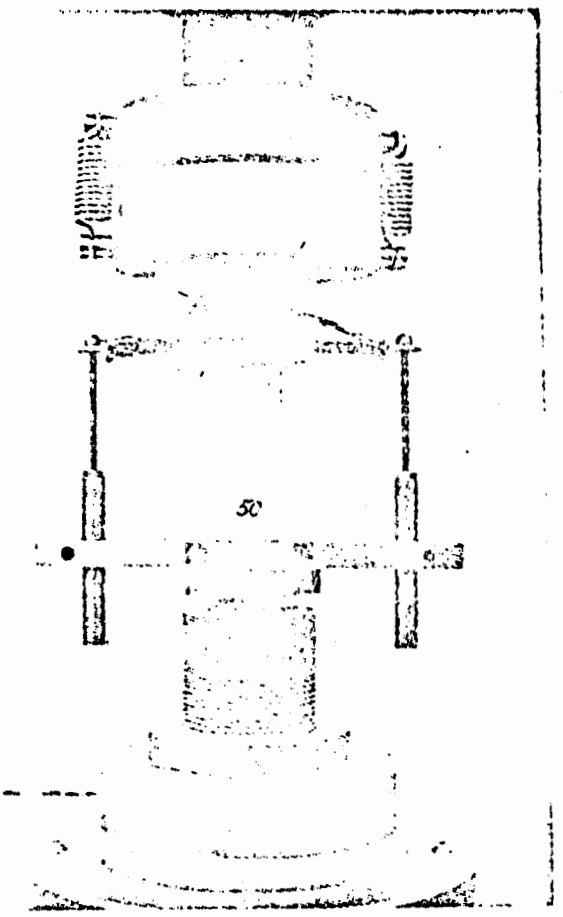

FIG. 2 LOADING JIG WITH SPECIMEN, CANTILEVER SET AND SWIVEL HEAD.

The platens had a diameter only slightly larger than that of the specimens and were part of a loading jig especially built fot these tests. The lower platen was rigidly attached to the hydraulic ram; the upper platen contained a swivel head mechanism to ensure that complete contact was made with the specimen. To prevent slippage of the swivel head, six bolts were used to lock it to the part of the loading jig rigidly attached to the crosshead. The locking of the bolts was a tedious job, carefully performed to ensure good alignment between specimen and platens. Overtightening of one of the bolts could cause misalignment and hence premature failure in cyclic testing. Utmost care was, however, taken in specimen installation

and the consistency of the results testify to the success of the method.

Experimental Program

The portion of the fatigue testing program that has been carried out so far, and is described in this paper, was limited to uniaxial compression. The intent was to test rock cylinders under compressive loading increased steadily from zero load to a certain upper peak, decreased at the same rate to the initial point, and cycled until failure occured. To prevent loss of contact between sample and platens at zero load, the lower peak of the compressive cycle was moved up to around 200 psi and was kept approximately constant throughout the testing program. The upper peak, however, was set anew for each test.

The cyclic rate used was intended to simulate the frequencies of the major pulses in earthquakes (1-2 cps) and blasting (10 cps). In the tests described the frequencies were kept at 1-4 cps. The higher frequencies were preferred because of shorter test duration, but the lower frequencies (1-2 cps) were necessary when stress-strain recordings were made, due to the X-Y plotter response limitations. The maximum number of cycles per test was kept at 10^6 with a few exceptions when the figure was exceeded. To obtain a representative S-N curve the fatigue life of specimens (number of cycles to failure) was determined for different upper-peak stress values. The general procedure was to reduce the maximum applied load from test to test until the fatigue life of the specimens reached 10^6 cycles.

Cyclic tests were also run on specimens that had been first loaded up to their peak compressive stress carrying capacity. In Georgia Marble, specimens were actually brought to 70% of the peak stress capacity on the descending side of the complete stress-strain curve, and only then cyclicly loaded. In order to test the fatigue characteristics of these failed specimens quasi-static strain-

controlled loading was used to bring the rock to the initial condition for cyclic stress-controlled loading.

EXPERIMENTAL RESULTS

The most extensive testing in the program has been carried out in White Tennessee Marble. The first stage of the experimental work was to determine the compressive strength of the rock, a value to be used as the upper limit to the maximum applied stress in cyclic loading. Specimens were loaded stress-controlled, at four different rates, two in the quasi-static range, and two in the dynamic range used in the cyclic loading. The results (Table 1) show that the

TABLE 1.--COMPRESSIVE STRENGTHS OF WHITE TENNESSEE MARBLE AT DIFFERENT LOADING RATES

Loading rate (psi/sec)	No. of Specimens	Mean Compressive strength (psi)	Standard Deviation	
			psi	%
40	9	19,740	355	1.8
100	11	21,150	900	4.2
50,000	12	23,285	840	3.6
200,000	7	24,890	425	1.7

compressive strength varies considerably with the rate of loading. Hence, whenever this parameter is employed it should be accompanied by the conditions under which it was determined. Because of the high response required, a storage type oscilloscope was employed to directly record the stress strain curve in each of the tests. By photographing the oscilloscope trace a permanent record was obtained.

The first important conclusion drawn from cyclic testing of White Tennessee Marble is that it is definitely weakened by repetitive loading. The fatigue effect can best be verified from the S-N curve shown in Fig. 3. The stress is given in percentage of the compressive strength

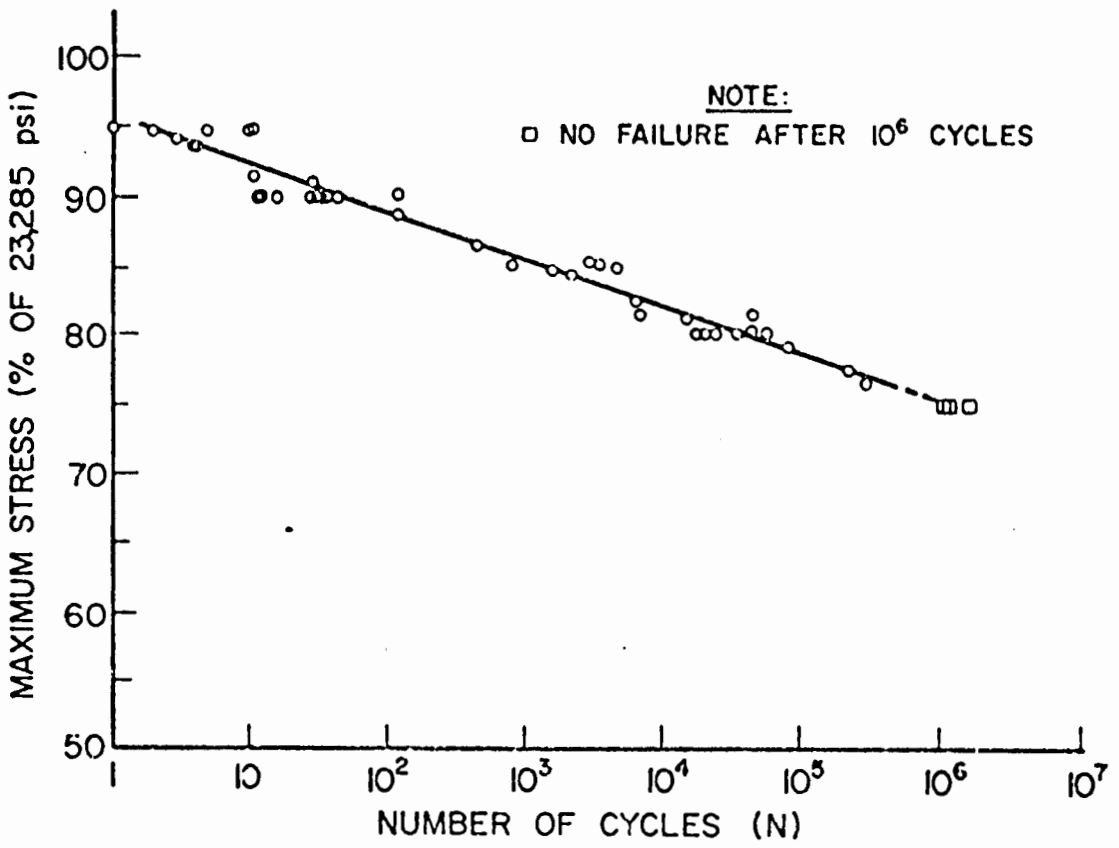

FIG. 3 S-N CURVE FOR WHITE TENNESSEE MARBLE

at 50,000 psi/sec. Most of the tests were run at 4 cps, while some were run at 1 or 2 cps for the purpose of recording stress-strain characteristics. No apparent difference was found between the frequencies used as far as specimen fatigue life was concerned. The S-N curve clearly shows that as the maximum compression decreases the life expectancy of a specimen increases. Fig. 3 also indicates that the spread of experimental points was surprisingly limited, due to the uniformity of the rock as well as the great care taken in the preparation and operation of the tests. In a semi-logarithmic plot, as the one shown in Fig. 3, the average relationship between the maximum applied stress (S) and the number of cycles needed to cause failure (N) is given by a straight line. At 75% of the dynamic

compressive strength used specimens did not fail within the experimental limit of 10^6 cycles. Moreover, when loaded monotonically to failure at the conclusion of the cyclic test, they did not show any sign of weakening or strengthening effects. It is hardly expected that rock will be subjected to a larger number of similar loading cycles during the expected life of an engineering structure. In an earthquake, for example, no more than 100-200 cycles are encountered (2). Hence, the value of 17,450 psi (=0.75 x 23,285 psi) can be used as the fatigue limit or the critical compressive strength of White Tennessee Marble. A design in intact rock using this value, not only is protected against static and dynamic stresses but also against all kinds of cyclic loading.

Typical stress strain cruves are shown in Fig. 4. Permanent

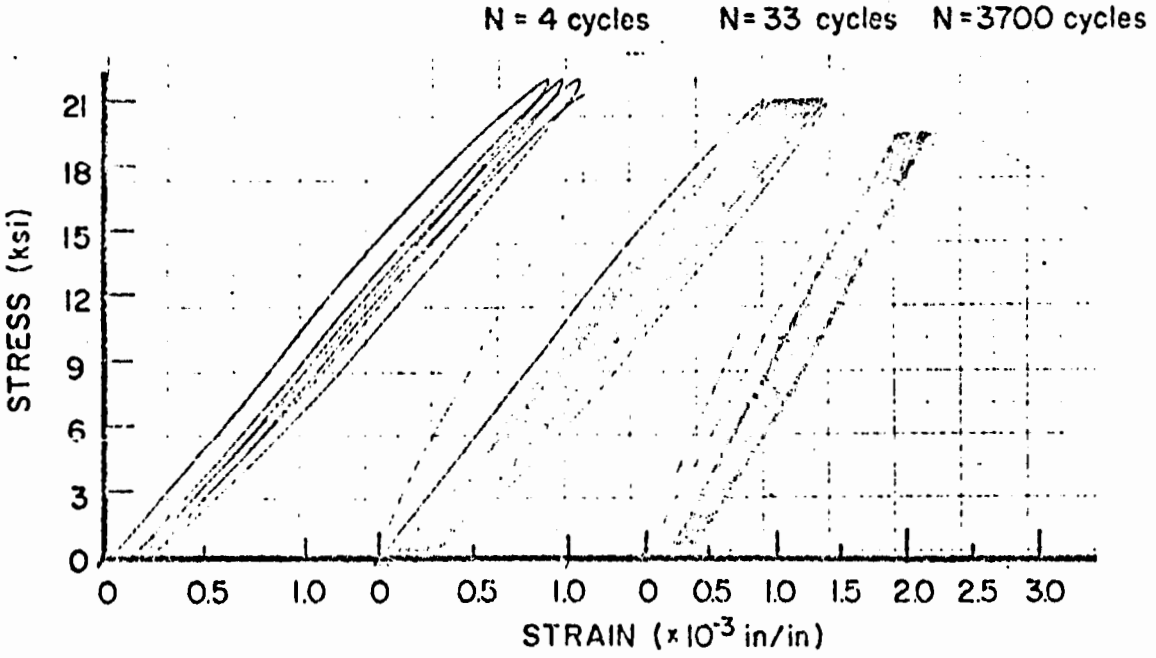

FIG. 4 STRESS-STRAIN CURVES FOR WHITE TENNESSEE MARBLE CYCLICLY LOADED TO DIFFERENT MAXIMUM STRESS VALUES

strain appears to accumulate in the rock with the dissipation of a relatively high amount of energy. Common to all tests is the phenom-

enon of rather large hysteresis in the first few cycles, an almost complete closure in the next group of cycles, and a reopening in the last several cycles prior to failure. The hysteresis in the first cycles is probably due to the very high peak loads which take the rock to beyond its linear elastic limit and into the zone of irreversible structure changes. In the very short life tests, the damage done by the high stresses is irreparable and the specimens break before reaching the second stage. For lower applied maximum stresses the phenomenon of hysteresis closure occurs seemingly due to micro-crack propagation being blocked and the linear elastic limit being lifted. As cyclic loading continues, the actual fatigue phenomenon eventually takes place, internal cracking reinitiates, the hysteresis grows and the specimen finally fails.

The amount of strain difference between the upper peaks of the last and first stress-strain cycles has been closely followed. No hard conclusions can be drawn as yet, but it appears that it is definitely limited by the strain difference between the ascending and the descending parts of the complete stress-strain curve for the same value of stress. This implies that the complete stress-strain curve actually defines the limit of strain that can be applied to a rock at a certain stress level, without producing failure. Quantitatively, the amount of strain difference varied between 25 - 35 x 10^{-5} inch/inch, which is within the limit set by the complete stress-strain curve.

The behavior of strain versus time was often recorded and a typical result is shown in Fig. 5. The curve shaped by the upper peak points clearly resembles that of creep behavior, and can be divided into three stages. There is a primary stage in which the upper peak strain increases at a decelerating rate. It is followed by a steady state stage which appears in Fig. 5 as an ascending straight line. In medium and long life tests this stage is invariably the longest. The third and final stage is that of accelerating upper peak strain culminating in specimen failure. The stages observed in the strain-time

behavior match those in the stress-strain characteristics.

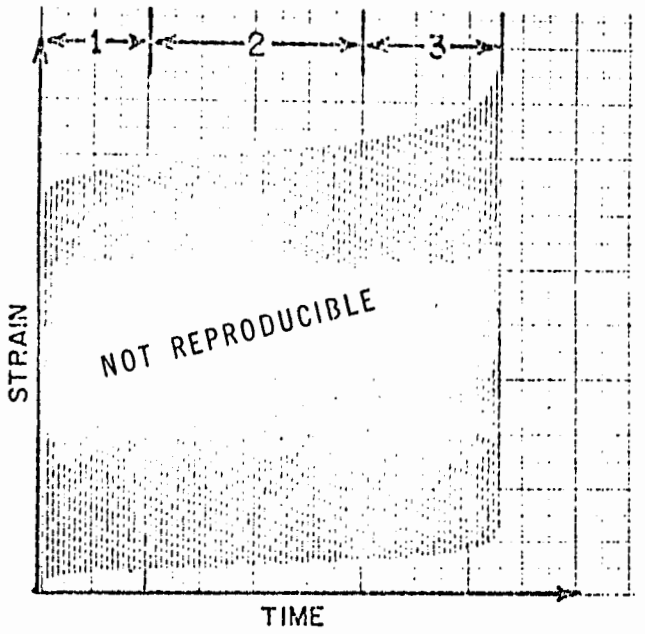

FIG. 5 TYPICAL STRAIN-TIME CURVE

It can be easily verified from Fig. 5 that the lower peak strain points undergo a much more reduced amount of increase. This implies that the value of the tangent modulus per cycle generally decreases during the test. Indeed, the average modulus of the ascending portion of the first cycle was 11.1×10^6 psi, while that of the last cycle was 9.9×10^6 psi. Similar results had been found in concrete (5).

Typical fatigue failed specimens are shown in Fig. 6. No apparent external difference was found between this type of failure and that encountered in quasi-static loading. Several samples were removed from the loading machine during different stages of the cyclic loading. The samples were vertically sectioned, polished and photographed. No damage was observed in specimens that had not reached the accelerated strain increase stage. Those that had reached the last stage prior to failure showed extensive structural damage dominated by vertical cracking. A photomicrograph of the central part of a vertical

section in a specimen removed during thelast stage is presented in Fig. 7.

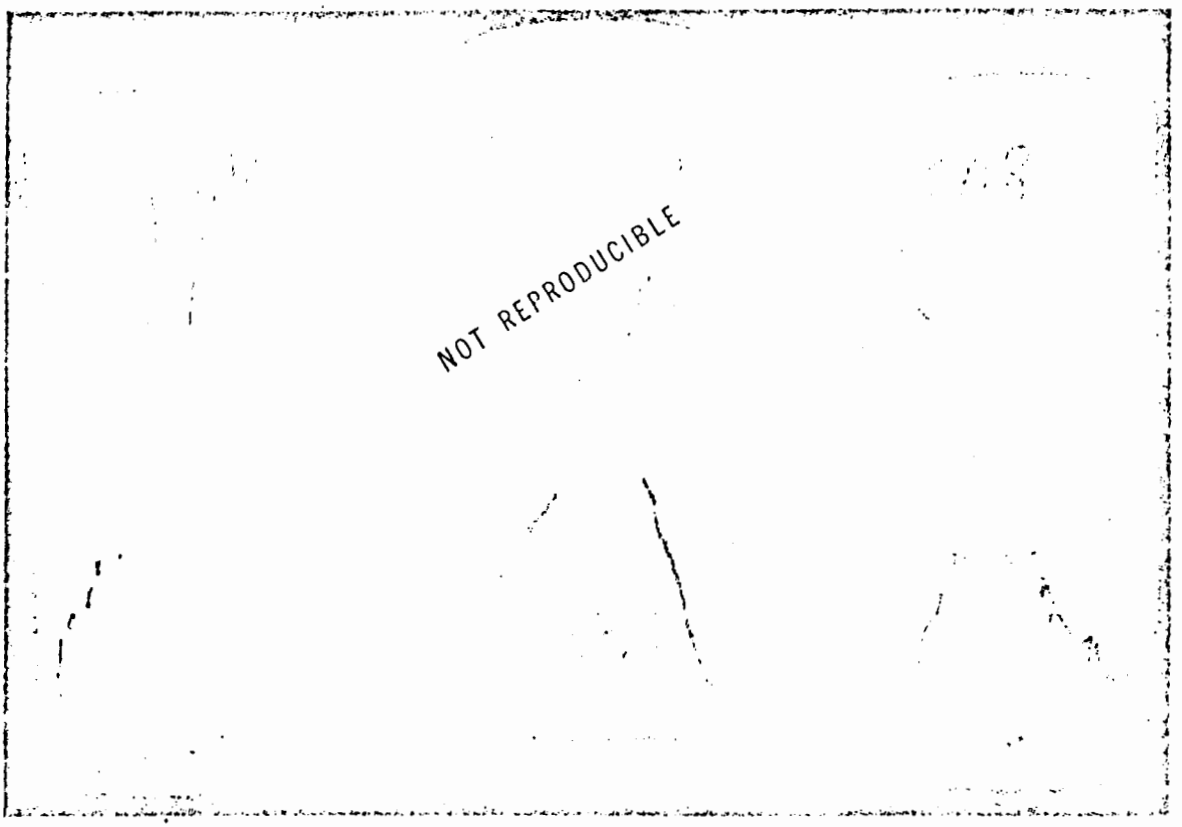

FIG. 6 FATIGUE FAILED WHITE TENNESSEE MARBLE SPECIMENS

A series of cyclic loading tests was run in White Tennessee Marble that had first been loaded in strain control to its compressive stress carrying capacity limit. This is the value commonly referred to as the compressive strength. In stress-controlled loading rock specimens will fail violently at this point as they cannot take any additional compressive force. However, if the loading is performed by controlling strain rate the rock will not collapse as it can usually continue to shrink in length while its load supporting capacity is gradually lowered. In this fashion a complete stress-strain curve can be obtained. Fig. 8 shows such a curve in addition to four other plots. In each of the plots a specimen was loaded up to its compressive strength, unloaded, and then cycled

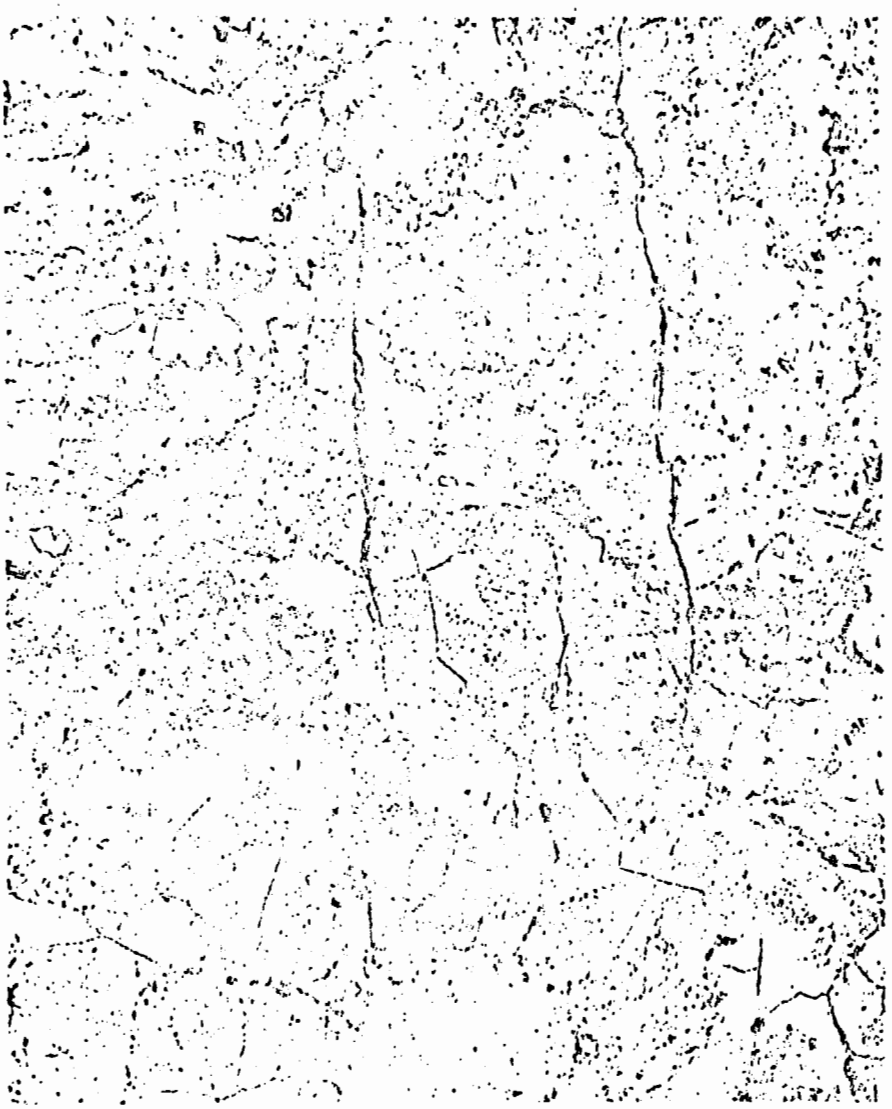

FIG. 7 PHOTOMICROGRAPH OF A FATIGUE FAILED SPECIMEN--VERTICAL SECTION

in stress control to an upper peak value lower than the ultimate strength. The purpose was to verify whether such failed rock could support fatigue type loading. Surprisingly the rock appeared rather strong, and could probably still perform useful work, although a comparison with the S-N curve in Fig. 3 will show that it had considerably weakened. As expected, the number of cycles increased as

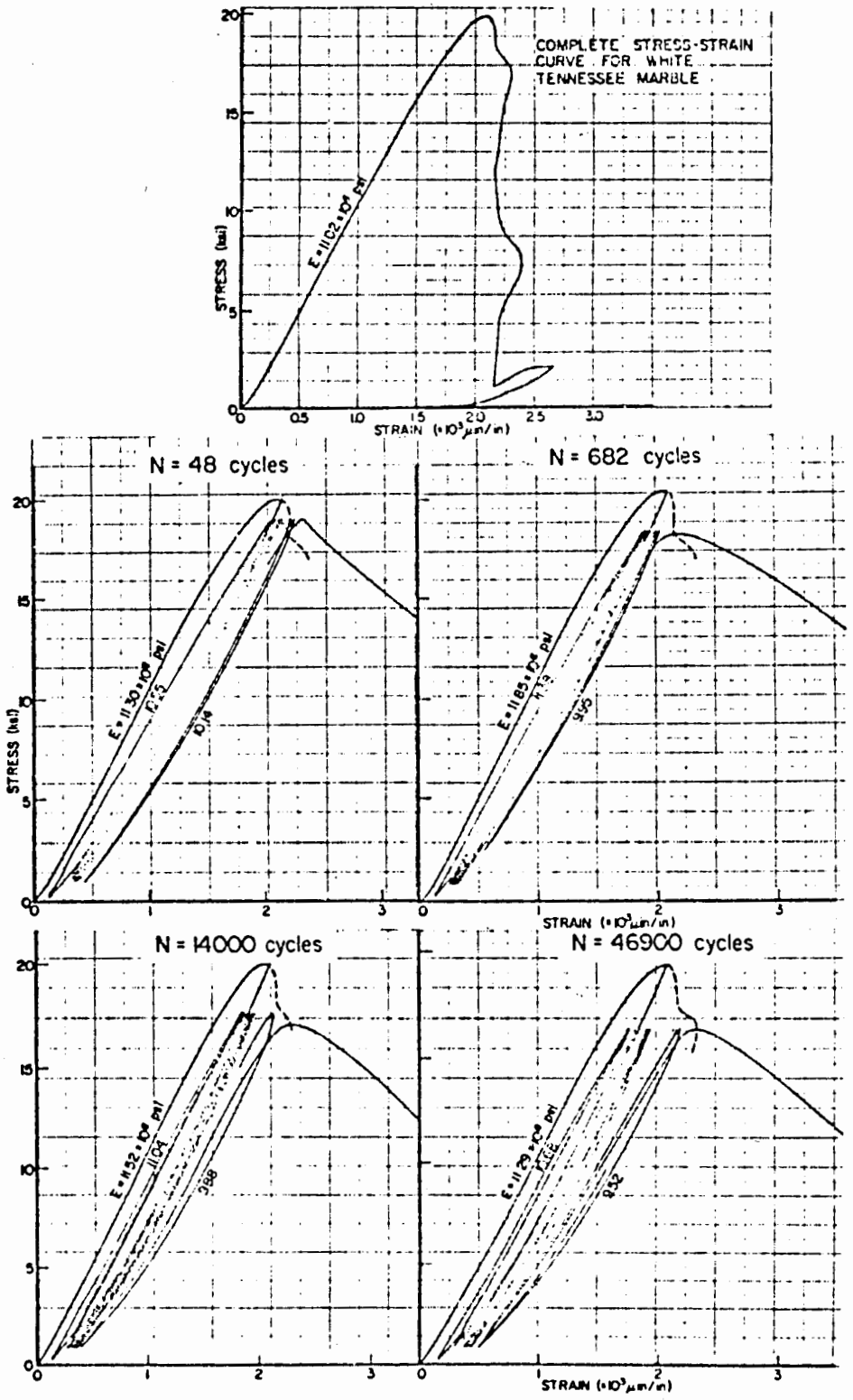

FIG. 8 STRESS-STRAIN CURVES FOR FAILED WHITE TENNESSEE MARBLE (DASHED LINES ARE EXPECTED COMPLETE STRESS-STRAIN CURVES)

the maximum applied load decreased. A close look at Fig. 8 will show that in three of the four plots the upper peak of the last cycle was in the close proximity of the expected descending line of the complete stress-strain curve. This was in accordance with the hypothesis raised above regarding the extent of the upper peak strain increase during cyclic loading.

An additional series of tests was contemplated well within the failed region characterized by the descending part of the complete stress-strain curve. Due to the very steep descending stress-strain curve in White Tennessee Marble, a different rock, namely Georgia Marble, was chosen for these tests. As seen in Fig. 9 the slope of the failed portion of the curve is very mild in the latter rock. This enabled one not only to obtain repeatable complete stress-strain curves, but also to stop the loading at any point in the failed zone and unload without the danger of specimen collapse. Georgia Marble specimens were loaded in strain control to their compressive strength and beyond, to 70% of the load carrying capacity within the failed zone. They were then unloaded, and cyclicly loaded in stress control to upper peak values of different magnitudes. The results are shown in Fig. 9. A preliminary S-N curve based on these tests is shown in Fig. 10. Again, one is surprised to note that failed rock can still show remarkable strength as far as cyclic loading carrying capacity. It is emphasized again, however, that for the same peak loads in the unfailed mode the number of cycles would be appreciably larger. Moreover, it is clear that in both rocks the fatigue limit is lowered in failed rock. It can be noted from Fig. 9 that the upper peak of the last cycle falls again in the close proximity of the expected descending complete stress-strain curve. The behavior of failed rock under cyclic loading is of particular importance to the understanding of failed underground pillars and walls subjected to fatigue type stresses. Because failed rock is internally fractured, the study may also be indicative of the behavior of jointed benches or slopes and faulted

formations subjected to earthquake, blasting, or traffic loadings.

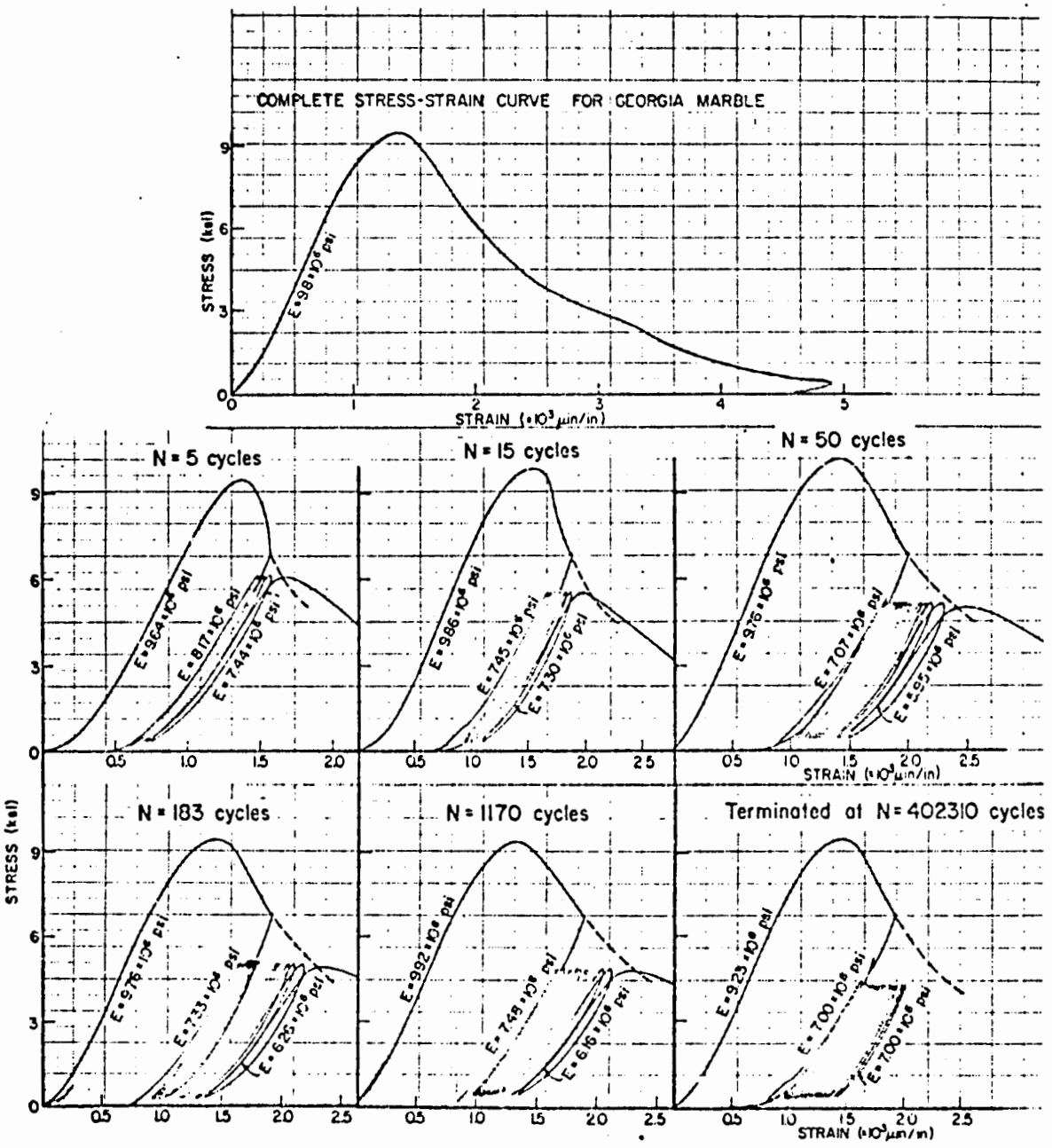

FIG. 9 STRESS-STRAIN CURVES FOR FAILED GEORGIA MARBLE
(DASHED LINES ARE EXPECTED
COMPLETE STRESS-STRAIN CURVES)

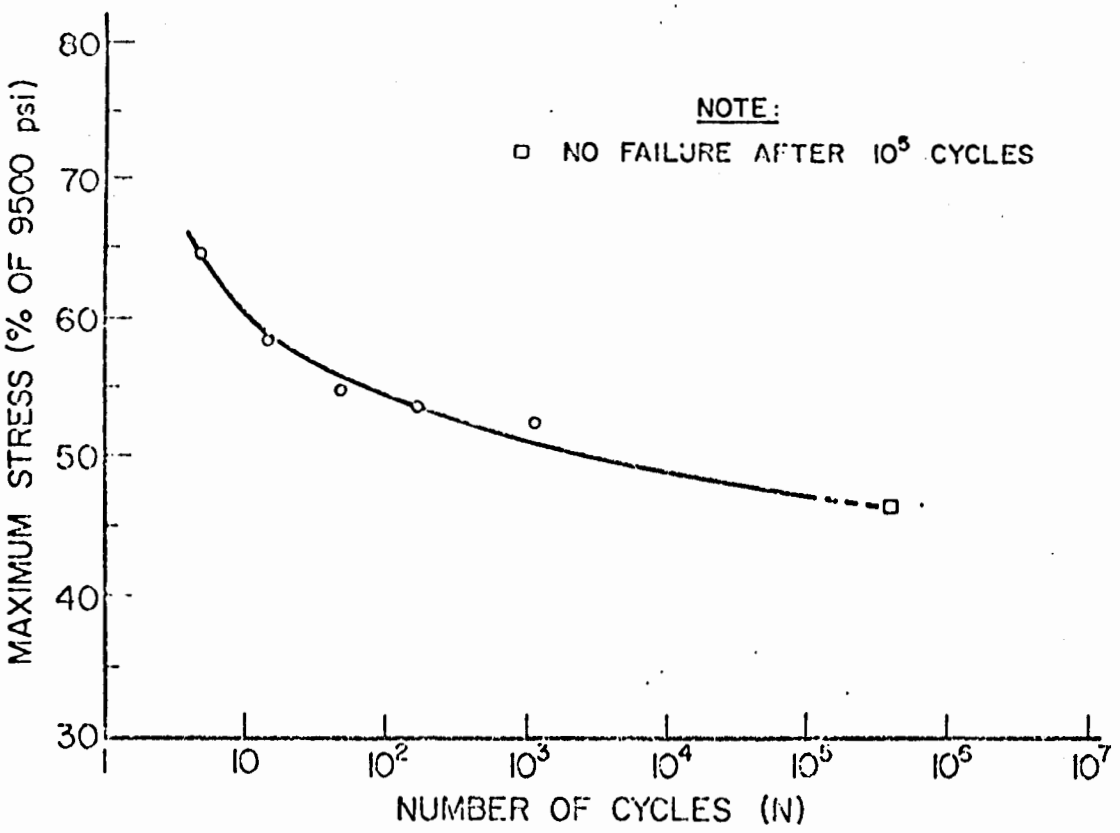

FIG. 10 S-N CURVE FOR FAILED GEORGIA MARBLE

SUMMARY AND CONCLUSIONS

The work reported here is only the first phase of an extensive investigation into the behavior of rock under cyclic loading. The main results obtained thus far in cyclic uniaxial compression of White Tennessee Marble are:

1) Cyclic loading has a definite weakening (fatigue) effect on the rock if the maximum applied stress is in the 75-100% range of the compressive strength.

2) Stress-strain records reveal three major stages occuring during cyclic loading: decreasing hysteresis, no hysteresis, increasing

hysteresis. The last stage is associated with fatigue affected internal fracturing.

3) The increase in upper peak strain between the first and the last cycles is always within the limit set by the complete stress-strain curve for the same maximum applied load.

4) The variation of the cyclic upper peak strain with time closely resembles that of creep, with primary, steady state, and tertiary or accelerated stages.

5) No visible structural damage can be observed in specimens removed prior to the accelerated strain-increase stage. However, polished sections of specimens that had reached the tertiary stage show an abundance of internal fracturing dominated by vertical cracking along and across grain boundaries.

6) Failed rock, although weakened, can sustain a certain amount of fatigue loading depending on the level of applied stresses. This conclusion is supported by testing of both Tennessee and Georgia Marbles.

The results obtained thus far show that rock cyclic fatigue is a phenomenon that cannot be ignored by engineers and rock mechanics scientists. A direct recommendation emerging from the study is that in surface and underground design the apparent fatigue limit, as determined by tests similar to those described above, be used instead of the commonly employed compressive strength value. In the design of structures that eventually reach their peak load carrying capacity, use could be made of the fatigue characteristics of failed rock. These characteristics are believed to also be indicative of jointed and faulted rock behavior under cyclic loading. The mechanism of fatigue is not yet clearly understood but the findings are promising enough to justify continuation of the research. Studies on the behavior of rock in uniaxial compression, tension and triaxial compression subjected to cyclic fatigue are currently underway.

ACKNOWLEDGEMENTS

The authors wish to acknowledge the financial assistance of the Wisconsin Alumni Research Foundation in the early stages of the investigation. The research was supported by the Advanced Research Projects Agency of the Department of Defense and was monitored by the United States Bureau of Mines, Twin Cities Research Center, under contract no. H0210004. J. A. Hudson and F. Rummel, University of Minnesota, provided invaluable suggestions and assistance.

APPENDIX--REFERENCES

1. Burdine, N. T., "Rock Failure Under Dynamic Loading Conditions", Society of Petroleum Engineers Journal, March 1963, pp 1-8.
2. Ellis, Willard and Hartman, V. B., "Dynamic Soil Strength and Slope Stability", Journal of the Soil Mechanics and Foundations Division, A. S. C. E., vol. 93, No. SM4, July 1967, pp. 355-375.
3. Grover, H. J., Dehlinger, P., and McClure, G. M., "Investigation of Fatigue Characteristics of Rocks", Report by Battelle Memorial Institute to Drilling Research, Incorporated, Nov. 30, 1950.
4. Hardy, H. R., Jr. and Chugh, Y. P., "Failure of Geological Materials Under Low-Cycle Fatigue", Proceedings of the Sixth Canadian Symposium on Rock Mechanics, Montreal, Canada, May 1970.
5. Nordby, Gene M. "Fatigue of Concrete--A Review of Research", Journal of the American Concrete Institute, Aug. 1958, pp. 191-219.
6. Wawersik, Wolfgang R., "Detailed Analysis of Rock Failure in Laboratory Compression Tests", thesis presented to the University of Minnesota, Minneapolis, in 1968, in partial fulfillment of the requirements for the degree of Doctor of Philosophy.